Received: 11 March 2026 | Revised: 10 August 2026 | Accepted: 12 August 2026

DOI: 10.1111/joa.70230

Journal of Anatomy | ANATOMICAL SOCIETY | WILEY

ORIGINAL ARTICLE

Heterodonty in the teeth of the turiasaurian sauropod from Angeac-Charente (Early Cretaceous, southwestern France): Comparison of anatomical and geometric morphometric approaches

Clémence L. E. Gouellec[1] | Ronan Allain[1] | Jean Goedert[1] | Romain Pintore[2,3] | Jackson Carter[1] | Rafael Royo-Torres[4] | Dominique Augier[5] | Raphaël Cornette[6]

[1]Muséum National d'Histoire Naturelle, Centre de Recherche en Paléontologie – Paris (CR2P), CNRS/MNHN/Sorbonne Université, Paris, France

[2]Institut des Sciences de la Terre de Paris, Sorbonne Université, CNRS, (UMR 7193 - ISTEP), Paris, France

[3]Institut de Physique du Globe de Paris, Université Paris Cité, CNRS, (UMR 7154 - IPGP), Paris, France

[4]Instituto Universitario de Ciencias Ambientales (IUCA-Beagle), Facultad de Ciencias Sociales y Humanas, Universidad de Zaragoza, Teruel, Spain

[5]Musée d'Angoulême, Angoulême, France

[6]Institut de Systématique, Évolution, Biodiversité "ISYEB" - UMR7205 - CNRS, MNHN, UPMC, EPHE, Sorbonne Universités, Université des Antilles Équipe: "Diversification et Adaptation aux échelles micro et macro-évolutives", Paris, UA, France

Correspondence
Clémence L. E. Gouellec
Email: clemence.legouellec@gmail.com

Funding information
ARS CUTTOLI, PAUL APPELL Foundation; Fundación Conjunto Paleontológico de Teruel-Dinópolis; DIM MAP région Iles de France

Abstract

Sauropod teeth are often described within a taxonomic framework, with few studies focusing on heterodonty or intraspecific morphological variation. The Lagerstätte of Angeac-Charente has yielded 167 heart-shaped isolated teeth from a single turiasaurian species. Observations of this material during its collection in the field, preparation, and recording in the collections suggest the presence of possible heterodonty in this species. In this study, we analyze this heterodonty using both comparative anatomy and 3D geometric morphometric analyses coupled with machine learning algorithms. Our principal objective is to determine whether one of the two approaches—quantitative or qualitative—is more effective than the other and whether they can be complementary studying heterodonty. The results confirm the presence of heterodonty, with five different morphotypes, which correspond to premaxillary, maxillary anterior, maxillary posterior, anterior dentary, and posterior dentary teeth. An anteroposteriorly decreasing size gradient in the jaw is observed. Qualitative comparative anatomy is the quickest method, with few conflicts in morphotyping, while quantitative approaches might resolve ambiguities through more precise and replicable analyses. Together, these methods provide complementary insights and allow retrospective positioning of teeth within the jaw. This study, therefore, allows for the reliable assignment of teeth to specific regions or positions in turiasaurian sauropods. Such assignment work is also necessary for many other taxa, and this method will, therefore, be useful for future research. Indeed, it is fully applicable to other sauropod taxa, theropods, or crocodilians.

KEYWORDS
3D geometric morphometrics, classification, comparative anatomy, dinosaur, heterodonty, machine learning, sauropod, teeth

1 | INTRODUCTION

In biology, classification is used to organize and categorize organisms based on their similarities, such as taxonomic classification (Crowson, 2017; Ereshefsky, 1997; Linnaei, 1735). In paleontology, these classifications were first based on comparative anatomy (Farber, 1975; Kardong, 2006; Nieuwland, 2024; Owen, 1846). On teeth, a qualitative approach is both long-standing and central, as it allows to identify new taxa (e.g., Allain & Aquesbi, 2008; Whitlock et al., 2010), to understand the morpho-functional and adaptive traits of certain interspecific and intraspecific anatomical features (e.g., Button et al., 2017; Maiorino et al., 2015), and to establish phylogenies (Livezey & Zusi, 2001; Zangerl, 1948). Extensive quantitative methods have subsequently been developed to study biological shape and its variations for classification purposes (Cheverud et al., 1983; Klingenberg, 2010), notably in paleontology (Ferrón et al., 2020; Pintore et al., 2023). In particular, geometric morphometrics has proved highly effective in distinguishing different taxa and morphotypes (Cardini et al., 2007; Caumul & Polly, 2005; Lawing & Polly, 2010). Geometric morphometrics enables the study of shape variations in a given population and has therefore been widely applied to several biological fields, including phylogeny and functional morphology (Gunz et al., 2005, 2009; Zelditch et al., 2012). Initially used for 2D objects (Slice, 2007), this approach is also well suited for 3D structures (Gunz et al., 2005; Gunz & Mitteroecker, 2013). In both paleontology and neontology, this method allows for the differentiation and classification of different morphotypes within a dataset of biological objects from higher taxonomic ranks (Gomes Rodrigues et al., 2018; Segall et al., 2023) to the interspecific (e.g., De Brito & Prestianni, 2021; Schmieder et al., 2015) and even intraspecific rank (Pintore et al., 2023; Robin et al., 2023; Yang et al., 2022).

More recent classification methods, such as machine learning, have seen significant development in the past 10 years and are increasingly used in evolutionary biology, ecology (Feltes et al., 2018; Kuzenkov et al., 2020; Lürig et al., 2021), geology (Baucon & De Carvalho, 2024), and paleontology (Yu et al., 2024). Machine learning refers to the process of fitting predictive models to data or identifying informative groupings within datasets (Greener et al., 2022). In paleontology, two-thirds of studies using artificial intelligence (AI) focus on microfossil and macrofossil classification, while the remaining studies focus on accelerating the segmentation of fossil computed tomography (CT) scans and prediction (Yu et al., 2024). AI classifications use a number of machine learning methods, such as Fourier analysis, Gaussian mixtures, k-Nearest Neighbor (k-NN) (Silverman & Jones, 1989), mixture discriminant analysis (Wills et al., 2023), C4.5 (Quinlan, 2014), and Random Forest (Breiman, 2001) algorithms. Other deep learning methods such as convolutional neural networks (CNN), which identify patterns across images and are the most commonly used in paleontology, or knowledge-based systems (KBS), which rely on object recognition by learning from model images, are also used to classify microfossils (Athersuch et al., 1994; Beightol & Conrad, 1988; Liu et al., 1994). The comparison between human intelligence and AI is becoming increasingly common in medicine (Deo, 2015; Rajkomar et al., 2019; Sidey-Gibbons & Sidey-Gibbons, 2019). For instance, certain medical analyses, such as tumor segmentation, are performed by both humans and AI systems to assess which approach is more effective. Porz et al. (2016) found that both approaches are complementary and rather similar. It is well established that AI outperforms human capabilities in terms of speed, particularly in calculations and the management of large datasets (Korteling et al., 2021). Human intelligence performs better in solving problems related to sociology, empathy, object recognition and image analysis, but is subject to various biases that AI can avoid, such as confirmation bias (Korteling et al., 2021). In paleontology, the application of AI helps reduce the confirmation bias or misinterpretation that can occur during classification analysis. For example, AI-based classifications have been performed using supervised classification algorithms (i.e., with a training set) on pollens (Kaya et al., 2013), or on theropod and ornithischian footprints (Lallensack et al., 2022), and on theropod teeth (Wills et al., 2023). In this latter case, the machine learning classification model seems to provide more accurate classifications than humans based on image recognition (Yu et al., 2024). Furthermore, to reduce biases in taxonomy and cladistics, semi-supervised or even unsupervised machine learning can facilitate the identification of synapomorphies and diagnostic features and thus uncover previously hidden taxonomic relationships (Hou et al., 2023; Liu et al., 2023; Yu et al., 2024). In this context, comparing the effectiveness between human and AI classification of paleontological objects represents a relevant approach for future paleontological studies.

In this study, we examine the contribution of comparative anatomical classification, 3D geometric morphometrics (3D GMM), and machine learning-based classification to the study of intraspecific heterodonty in sauropods. We also seek to determine the extent to which these qualitative and quantitative approaches are complementary. We investigate which methods are the most time-consuming and the most challenging to implement. The goal is to determine whether these two complementary methods are truly effective, which would make it possible to apply them to other studies. To answer these questions, we studied a sample of 167 isolated sauropod teeth belonging to the Turiasauria indeterminated taxon from the Early Cretaceous Lagerstätte of Angeac-Charente, recovered during the annual excavation campaigns from 2010 to 2024 (Allain et al., 2022). We analyzed these teeth using a combination of comparative anatomy and 3D GMM coupled with machine learning classification in order to investigate tooth shape variation within this taxon and to assess whether distinct morphotypes could be identified and anatomically associated with the three tooth-bearing jawbones (premaxilla, maxilla, and dentary), as well as with more anterior or posterior positions within the jaw.

1.1 | Heterodonty and homodonty in amniotes

Classically, heterodonty refers to teeth of different shapes or morphologies, typically associated with functional differentiation.

Heterodont dentition often reflects dietary specialization, with distinct tooth types adapted to specific roles in food processing (Maier, 1984). It has been highly documented in mammals, which in general have highly differentiated teeth (incisors, canines, premolars, and molars) (e.g., Yamanaka et al., 2015). In fact, this is the classic definition of heterodonty: the presence of discrete dental categories. Nevertheless, some mammals are secondarily homodont, such as odontocetes and early-branching mysticetes, which possess simplified, uniform teeth along the dentary row (Armfield et al., 2013). In contrast, homodonty refers to a dental pattern where all teeth within the jaws exhibit a similar morphology. Among amniotes, homodont dentition is most commonly associated with reptiles (Zahradnicek et al., 2014). A classic homodont model has been observed in several squamates such as in the snake *Python molurus*, in the gecko *Paroedura picta* and in the Monitor lizard *Varanus niloticus* (D'Amore, 2015; Zahradnicek et al., 2014). However, heterodonty in relation with diet is observed across various reptile clades, both in extant and extinct species (e.g., Lafuma et al., 2021; Melstrom, 2017). For instance, the anole *Anolis allisoni* is described as heterodont in Zahradnicek et al. (2014), and in snakes, jaws can be composed of several tooth morphotypes, related to dietary specialization (Segall et al., 2023). Heterodonty is also present in Rhynchocephalia, in which fossil and extant clades show several tooth shapes and sizes on marginal bones, particularly in herbivorous forms (Chambi-Trowell, 2024).

In archosaurs, many heterodont jaws are also found among crocodilians. For instance, the Nile crocodile exhibits heterodont dentition (Fruchard, 2012; Kieser et al., 1993). Additionally, a transition from caniniform to molariform teeth has been identified in several groups of both extant and fossil crocodilians (Erickson et al., 2012, 2014; Gignac & Erickson, 2014). D'Amore et al. (2019) explain that their heterodonty is characterized by variability along the dentary row, with tooth shape being strongly influenced by the position in the jaw. Whereas some extinct herbivorous crocodilians were heterodont (D'Amore et al., 2019), the above observation of heterodonty challenges the long-standing notion that non-herbivorous crocodiles were homodont (Langston, 1973; Larsson & Sidor, 1999; Osborn, 1998; Zahradnicek et al., 2014).

In dinosaur paleontology, teeth are among the most frequently recovered fossils and are well suited for both qualitative and quantitative studies. Numerous biometric studies on theropod teeth have already been conducted (Farlow et al., 1991; Farlow & Brinkman, 1994; Hendrickx et al., 2015a, 2020; Larson & Currie, 2013; Smith, 2007; Smith et al., 2005) as well as more recent studies using 2D GMM (Buckley et al., 2010; Buckley & Currie, 2014; Hendrickx & Mateus, 2014). These teeth are almost always studied (Hendrickx et al., 2015a) in an attempt to achieve taxonomic identification, often at the subclade level (Hendrickx et al., 2020; Smith et al., 2005). Sauropods had a high tooth replacement rate (D'Emic et al., 2013; Sereno et al., 2007). As a result, they shed multiple generations of teeth throughout their lives, making the discovery of isolated rootless teeth particularly common in Mesozoic sediments. Dinosaurs have long been considered homodont; however, this notion is now considered outdated, as heterodonty appears to be far more common among reptiles (D'Amore et al., 2019; Norman et al., 2011; Segall et al., 2023; Sereno, 2012). Homodonty is present in many dinosaur clades; for instance, among ornithischians, ceratopsians like *Protoceratops* and *Triceratops* have uniform teeth arranged in dental batteries (Nabavizadeh, 2023; Ostrom, 1966). Similarly, among thyreophorans, all teeth are uniform, whether in ankylosaurs (Mallon & Anderson, 2014) or stegosaurs (Reichel, 2010a, 2010b; Sereno & Zhimin, 1992). However, although homodonty predominates among ornithischians, there are exceptions. Heterodontosauridae, for example, exhibit incisiform teeth, a caniniform tooth, and a mesiodistally decreasing size gradient along the jaw (Norman et al., 2011; Sereno, 2012). Euornithopods (i.e., Ornithopoda except *Heterodontosaurus*), particularly *Iguanodon*, show slight heterodonty, with slight morphological differences observed between maxillary and dentary teeth (Kobayashi & Azuma, 2003). Among saurischians, theropods are better described as pseudo-heterodonts, as tooth morphology changes gradually along the jaw (Hendrickx et al., 2015a, 2015b). This heterodonty is clearly observed in *Tyrannosaurus rex*, which exhibits several dentary morphotypes (Osborn, 1905; Reichel, 2010b; Smith, 2005). Spinosaurids show heterodonty similar to that found in crocodilians (D'Amore et al., 2024; Vullo et al., 2016). It is also evident in other theropod groups, such as abelisaurids and megalosaurids (Hendrickx et al., 2015a; Smith, 2007). However, homodonty is also found among theropods, as exemplified by *Carcharodontosaurus* (Smith et al., 2005).

In sauropods, dental morphology also allows taxonomic questions to be addressed (Torcida Fernández-Baldor et al., 2024; Wiersma & Sander, 2016). Biometrics analysis has been carried out to highlight taxonomic variations such as the measurement of the slenderness index (SI) (Frauenfelder et al., 2024; Mocho et al., 2016, 2017; Saleiro & Tschopp, 2025). Comparative anatomy and biometric analyses distinguish different dental morphotypes in sauropods at various taxonomic levels (Barrett & Upchurch, 2005; Holwerda et al., 2015; Mocho et al., 2016, 2017; Saleiro & Tschopp, 2025). For instance, based on comparative anatomy, Mocho et al. (2017) identified four main morphotypes among sauropod teeth from the Upper Jurassic sediments of the Lusitanian Basin, subsequently used in other studies (Mocho et al., 2017; Royo-Torres et al., 2021; Saleiro & Tschopp, 2025; Torcida Fernández-Baldor et al., 2024). Two morphotypes are characterized by broad-crowned teeth: heart-shaped teeth (Mocho et al., 2017) and spatulate teeth (e. g., *Camarasaurus lentus*, Chure et al., 2010). The other two morphotypes correspond to narrow-crowned teeth: compressed cone-chisel-shaped teeth and pencil-shaped teeth. The Turiasauria indet. from Angeac-Charente, like other turiasaurs, has heart-shaped teeth (Allain et al., 2022; Royo-Torres et al., 2006, 2021). Heterodonty in both size and shape is clearly visible in *Camarasaurus* (White, 1958; Wiersma & Sander, 2016) as well as in Turiasauria (Britt et al., 2017; Mocho et al., 2016, 2017; Royo-Torres et al., 2006, 2017, 2021; Royo-Torres & Upchurch, 2012; Saleiro & Tschopp, 2025). A slight heterodonty is also present in Brachiosauridae (Christiansen, 2000; Liao et al., 2021).

In contrast, the dentitions of the clade Diplodocoidea, with jaws possessing dental batteries (Christiansen, 2000; Whitlock et al., 2010), and Titanosauria (Rogers & Wilson, 2005; Wilson, 2005) are homodont. To date, only two studies using geometric morphometrics have explored the interspecific morphological variation of sauropod teeth (Ribeiro et al., 2024; Ribeiro Relvas, 2023). Furthermore, to our knowledge, intraspecific morphological variation in sauropod teeth is only addressed to highlight the classification of teeth according to jawbone. Moreover, it has only rarely been studied in theropods (Buckley et al., 2010; Buckley & Currie, 2014).

2 | MATERIALS AND METHODS

2.1 | Dental material of Turiasauria indet. and data collection

Apart from the recent discovery in 2024 of the remains of a single sauropod individual with anatomical features diagnostic of the basal macronaria clade (Ronan Allain (RA) and Rafael Royo-Torres (RRT) pers. obs.), all sauropod material from Angeac-Charente discovered since 2010 shares many anatomical features with the Late Jurassic Spanish turiasaurs *Losillasaurus giganteus* and *Turiasaurus riodevensis* (Néraudeau et al., 2012; RA and RRT pers. obs.) and was therefore assigned to Turiasauria indet. (Allain et al., 2022). Of all the sauropod teeth recovered from Angeac-Charente sediments, only two have been attributed to Macronaria indet. (Allain et al., 2022: *fig. 24 Y-AA*).

All recovered teeth share the dental characteristics typical of turiasaurs, namely heart-shaped, asymmetric teeth with a concave lingual surface and a convex labial surface at the crown, as well as an anterior projection of the mesial carina (Britt et al., 2017; Foster et al., 2026; Mateus et al., 2014; Milàn & Mateus, 2023; Mocho et al., 2016; Royo-Torres et al., 2006, 2017, 2021; Royo-Torres & Upchurch, 2012; Sharma et al., 2022). The Angeac-Charente Lagerstätte is a fossil site of modest extent (1200 m^2) and represents a snapshot of a Lower Cretaceous ecosystem, with sedimentological and taphonomic evidence of "frozen scenes" (Néraudeau et al., 2012; Rozada et al., 2021). Moreover, most of the teeth preserve their roots, or fragments of roots, suggesting that they were functional and, therefore, that the animals died at the site. No anatomical differences in the skeletal remains or teeth, discovered between 2010 and 2023, that might suggest the presence of two species of turiasaurians have been identified. All these elements support the interpretation that these teeth belong to a single taxon.

The dental material referred to Turiasauria indet. consists of 167 isolated teeth and a few fragmentary jaw bones found between 2010 and 2024. None of these jaw bones had functional teeth still in place, but they did have several in situ unerupted replacement teeth. The fragmentary nature of this material prevents the unambiguous determination of the exact number of functional (i.e., unshed) teeth based on the preserved tooth sockets that bear the premaxilla, maxilla, and dentary. Nonetheless, an incomplete right maxilla (ANG12-1908) preserved 13 tooth sockets, which is coherent with the condition observed in *Losillasaurus giganteus* (Royo-Torres et al., 2021). All of this material is housed and registered at the Angoulême Museum (Charente, France) under collection numbers ANG XX-YYYY, where ANG refers to the locality of Angeac-Charente, XX refers to the year of collection, and YYYY refers to the collection number.

Only the best-preserved tooth specimens (i.e., 137 teeth) were scanned using a handheld Artec Spider surface scanner. One hundred and thirty-seven 3D files were created and then edited in the ArtecStudio 18 Professional software (© 2024 Artec Europe), to make them usable for further use. The raw data were scaled, oriented, and contrasted to visualize the desired objects. The image resolution was then reduced to 8 bits and binned six times to obtain a lighter file and therefore facilitate faster processing. Of these 137 teeth for which 3D models are available, 114 teeth were considered by the various operators for anatomical comparison (see hereunder). Additionally, the incomplete right maxilla of Turiasauria indet. (ANG12-1908) was scanned using X-ray synchrotron microcomputed tomography (micro-CT) at the European Synchrotron Radiation Facility (ESRF Grenoble) in order to access the morphology of unerupted replacement teeth. Using the software Mimics v25.0 (©Materialise), the segmentation of the micro-CT scans of the right maxilla was performed to generate a 3D model of one of the unerupted replacement teeth. These 3D models ($n = 115$) were then further considered for GMM analysis.

2.2 | Comparative anatomy, human classification

Initially, in order to determine as precisely as possible the position of the teeth in the jaws, six operators with expertise in paleontology and those who were involved in the discovery of the material (R.

FIGURE 1 (a) Complete Turiasauria indet. tooth (ANG13-2330) of Angeac-Charente (scale = 2 cm) in labial, lingual, and mesial views (from left to right). (b) Interpretative drawing showing the seven morpho-anatomical criteria (italics) used by the operators for comparative anatomy classification. (c) Sauropod tooth template illustrating the landmarks (red dots 1–5), semi-landmark curves (blue dots, curves C1–C6′) and surface semi-landmark (green dots) used for 3D morphometric analysis. Landmarks correspond to clearly defined anatomical part of the tooth: 1—maximum curvature of the distal edge; 2—maximum curvature of the mesial edge; 3—lowest point of the cervix at the distal carina; 4—lowest point of the cervix at the mesial carina; 5—apex of the tooth; semi-landmarks curves connect these landmarks: C1—curve connecting point 1 to point 2 on the labial face; C2—curve connecting point 2 to point 1 on the lingual face; C3—curve connecting points 3 and 4 along the cervix on the labial face; C4—curve connecting points 4 and 3 along the cervix on the lingual face; C5—curve connecting points 5 and 1 along the apical part of the distal carina; C5'—curve connecting points 1 and 3 along the basal part of the distal carina; C6—curve connecting points 5 and 2 along the apical part of the mesial carina; C6′—curve connecting points 2 and 4 along the basal part of the mesial carina.

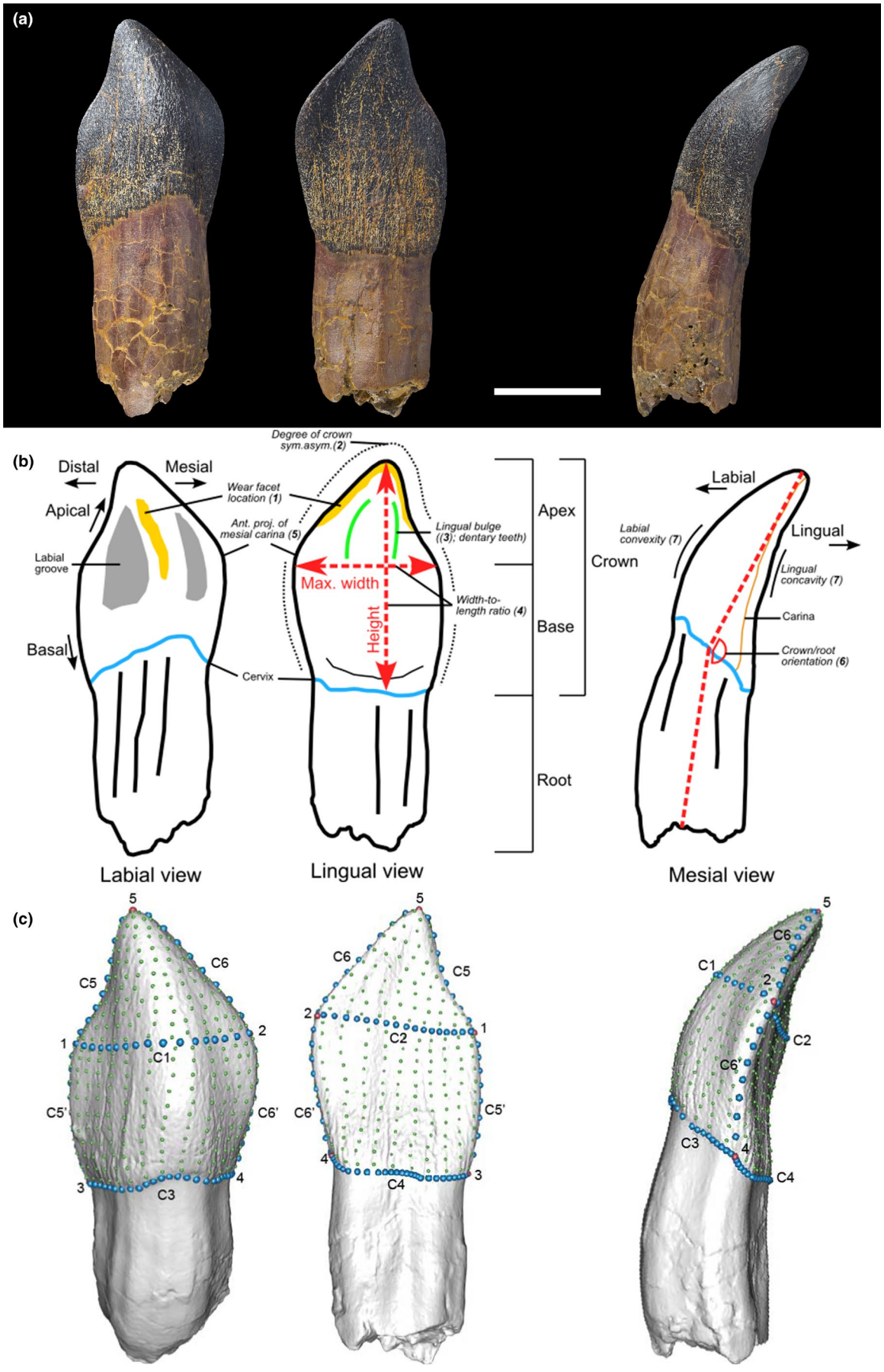
(a)
(b)
Distal
Mesial
Apical
Basal
Labial groove
Wear facet location (1)
Ant. proj. of mesial carina (5)
Degree of crown sym.asym.(2)
Lingual bulge ((3); dentary teeth)
Max. width
Height
Width-to-length ratio (4)
Cervix
Apex
Base
Root
Crown
Labial
Lingual
Labial convexity (7)
Lingual concavity (7)
Carina
Crown/root orientation (6)
Labial view
Lingual view
Mesial view
(c)
C1
C2
C3
C4
C5
C6
C5'
C6'

Allain (RA), D. Augier (DA), J. Goedert (JG), C. Le Gouellec (CLG), R. Pintore (RP) and R. Royo Torres (RRT)) were given access to all dental material referred to Turiasauria indet. from the Angeac-Charente site ($n = 167$). Only teeth allowing for reliable anatomical interpretation—that is, those with (nearly) complete crowns and without extensive pyrite encrustation—were considered by the six operators ($n = 114$). They examined all tooth material and performed anatomical comparisons using the same anatomical terminology (Figure 1a,b). They attempted to identify distinct morphotypes among these isolated teeth, to assign them to one of the three jaw bones (premaxilla, maxilla, or dentary), to determine their precise locus within these elements, and to lateralize them.

With the exception of a few jaw bones containing non-visible replacement teeth, all Turiasauria indet. teeth from the Angeac-Charente site are isolated, and their original position within the jaw is therefore unknown a priori. In addition to their own paleontological expertise, the six operators relied on the work of Royo-Torres et al. (2021), which describes a new specimen of *Losillaurus giganteus* from the Late Jurassic of Spain. Since this specimen serves as a reference for determining positions, all operators are familiar with the material and have already observed it. In addition, when evaluating the teeth, the operators had access to illustrations, as well as 3D models of the teeth of *Losillaurus giganteus*. So far, this unique specimen is the only turiasaur for which the three tooth-bearing bones (premaxilla, maxilla, and dentary) and almost the whole dentition (premaxillary, maxillary, and dentary teeth) are known. The geographical and temporal proximity of these taxa to the Angeac-Charente turiasaur further suggests that they were closely phylogenetically related. We have therefore considered the numbers of premaxillary, maxillary, and dentary teeth of *Losillasaurus giganteus* (Royo-Torres et al., 2021) to be representative of the Turiasauria indet. from Angeac-Charente. All six operators therefore considered four teeth on the premaxilla (labeled 1 to 4), 13 on the maxilla (anterior teeth labeled 5 to 11 and posterior teeth 12 to 17), and 15 on the dentary (anterior teeth labeled 1 to 5, middle teeth 6 to 10, and posterior teeth 11 to 15). The divisions between anterior, middle, and posterior teeth are defined arbitrarily.

For each operator, an "observation" was then defined as the completion of the following three operations for one given tooth: (i) attribute an anatomical information to the tooth regarding its jawbone origin (premaxilla [PM], maxilla [M], or dentary [D]); (ii) determine its absolute position along the jaw ([1–4], [5–17], and [1–15], respectively); and (iii) lateralize it (right [R] or left [L]). As each operator made their observations independently of each other and at different times, the number of observations (n_{obs}) differs between operators. For instance, RRT ($n_{obs} = 88$) did not observe the dental material from 2022 and 2023. DA ($n_{obs} = 106$) and RP ($n_{obs} = 107$) did not observe the material from 2023. CLG, JG and RA made the same number of observations ($n_{obs} = 114$) covering all the tooth material from 2010 to 2023. The teeth of Turiasauria indet. recovered in 2024 ($n = 3$) were not included in this study.

Consequently, of the 114 teeth considered, 87 were examined by all six operators, 19 by five operators, one by four operators, and seven by three operators (Data S1). Additionally, one of the unerupted teeth from the maxilla (ANG12-1908), reconstructed in 3D from micro-CT scans, was presented to two of the operators (JG and RP) without disclosing its origin. This allowed for a blind identification of a tooth for which the anatomical assignment (maxilla), lateralization (right), and position (7) were already known.

Based on the total number of observations per tooth, we defined four categories of identification consistency: (i) "consensus" when all operators assigned the tooth to a same morphotype (premaxillary [PM], maxillary [M], or dentary [D]); (ii) "weak consensus" when at least 75% (but less than 100%) of the observations were consistent (e.g., 5/6, 4/5, or 3/4 matching identifications); (iii) "weak conflict" when at least 60% (but less than 75%) of the observations were consistent (e.g., 4/6, 3/5, or 2/3); and (4) "conflict" when the highest proportion of observations assigning the tooth to a given morphotype was equal to the proportion assigning it to a different morphotype.

At the end of this comparative anatomical work, each operator documented the protocol and anatomical criteria they used to assign each isolated tooth to a specific dental morphotype and jaw position, as well as to determine its lateralization. They recorded their observations in a table and these six different tables were aggregated into a single one to highlight the differences in classification between operators (Data S1). A factorial analysis of mixed data (FAMD) was then performed on the human classification data in order to highlight the significant differences in observations between operators and the prioritization of the anatomical criteria used to make these observations. This analysis was conducted in R using the *FAMD* function from the *FactoMineR* package v2.11 (Lê et al., 2008).

2.3 | 3D geometrics morphometrics

Of 115 3D tooth surface models, 60 were excluded from the analysis due to significant damage, such as a broken crown, pyrite encrustations on the tooth surface, or a partially preserved cervix region preventing proper landmark placement (Data S2). As a result, 55 3D tooth surface models are included in the analysis. Among these, 26 were mirrored using *Meshlab (v2022.02)* to standardize lateralization. To assess morphological variation, two 3D GMM analyses were conducted. The first analysis ($n = 55$) excludes the apical region of the crown due to the presence of wear facets that alter its original shape to a greater or lesser extent depending on its stage of development. The second analysis includes only teeth with complete crowns and no wear facets ($n = 21$) and therefore takes into account the apical region. On the corresponding PCA figures, there are only n-1 specimens of the template tooth, which is not represented on the graph. The landmark placement was performed on the 3D files using *Landmark v3_b6 editor* (*renamed as Checkpoint*, https://www.stratovan.com/blog/idav-landmark-editor-checkpoint). For each specimen, four anatomical landmarks (A1-2 and A3-4 designate apical and basal crown, respectively) and six sliding semi-landmarks along curves (C1-2, C3-4, and C5-6 designate crown apical, mesial, and distal curves, respectively) with sliding semi-landmarks

(following Gunz & Mitteroecker, 2013) were placed on the crowns of the teeth. For the second analysis, to take the apex into account, we added a single anatomical landmark A5 and semi-landmarks along curves C5′ and C6′. Single anatomical landmarks and sliding semi-landmarks along curves were consistently placed in the same order across all specimens (Figure 1c). Landmarks' coordinates are then extracted and their distribution is statistically investigated using R (R Core Team, 2022; RStudio version 2023.12.1). The steps of this analysis are to (i) perform a Procrustes analysis and (ii) visualize morphological variation using principal component analysis (PCA). A Procrustes analysis is a superimposition method used to render landmark configurations comparable throughout the Cartesian coordinate system. It highlights differences in shape between specimens by calculating shape residuals after optimally aligning the configurations through rotation, translation, and scaling (Rohlf & Slice, 1990).

We choose the tooth ANG13-2330 as the reference model for the analysis, and we positioned surface sliding semi-landmarks between the apical and basal curves on the surface to create a template that was then projected onto the remaining specimens (Botton-Divet et al., 2015). Then, we using the *createAtlas* function from the *Morpho* R-package (Schlager, 2017) to generate the template in R. The generated template configuration for sliding semi-landmark along curves is then automatically projected onto all of the specimens in the dataset using the *placePatch* function, also part of the *Morpho* package. Once the model points are projected onto all specimens, a series of relaxations minimizing the bending energy between the model configurations and all the other specimens was performed using the *relaxLM* function over five iterations. This interpolation method deforms the model mesh to fit each specimen (Gunz & Mitteroecker, 2013). Then, we applied a series of relaxations minimizing the bending energy between an average configuration and all specimens was performed using the *slider3D* function of the *Morpho* package with five iterations. The landmark configurations resulting from these steps can be used to carry out the PCA in order to investigate morphological variation. In R, the PCA was carried out using the *gm.prcomp* function from the *Geomorph* package (Adams et al., 2022). PCA analysis allows us to visualize the location of different teeth in morphospace and in particular to determine if they form clusters in statistically different regions of this space, thus representing different morphotypes. PCA analysis was conducted for the dataset with and without complete crown (apex excluded). Morphological differences corresponding to the three principal components (PCs) were assessed. The results corresponding to strict consensus and weak consensus are placed in colored convex hulls. Conversely, strict and weak conflicts are represented by black dots on the PCs. A consensus shape was created using the *mshape* function from the *Geomorph* package (Adams et al., 2022). Finally, to visualize deformations (Klingenberg, 2013) along the first three PCs, we used the *plot3D* function from the *Geomorph* package (Adams et al., 2022) as well as the *tps3d* function (Bookstein, 1989). To validate the results obtained with the PCAs, k-NN analyses with cross-validation, which is used to automatically optimize hyperparameters of the model and prevent overfitting, were conducted using the *knn.cv* function from the *class* package (Venables & Ripley, 2002). This approach makes it possible to determine the number of teeth that the algorithm classifies into the appropriate group, as defined by the human classification performed earlier. Canonical variate analysis (CVA) corresponding to PCAs of the datasets both with and without complete crowns were performed to minimize within-group variation and maximize between-group variation, respectively. This allows us to determine whether the groups identified in the PCAs are significantly separated. We used the *CVA* function (Klingenberg & Monteiro, 2005) from the *Morpho* package to accomplish this. Finally, to determine whether size is an important factor in dental determination, we performed multivariate analyses of variance (MANOVAs) on the centroid size for each specimen both with and without complete crowns using the *aov* and *pairwise.t.test* functions.

2.4 | Clustering analysis

Clustering analyses based on the 3D GMM results were performed not only to assess whether the groups determined through comparative anatomy by the operators could be recovered but also to determine whether teeth with conflicting classification among operators could be assigned to a group on a quantitative basis. First, we perform supervised clustering, where the groups, into which undetermined objects are to be classified, are known in advance. To do this, we use the k-NN model pretrained with non-conflicting dental determinations to make predictions on the sample of teeth without determinations. To accomplish this, we use the *knn* function from the *class* package (Venables & Ripley, 2002). The k-NN was performed with a K value of 3.

We then performed semi-supervised clustering, during which we specified the total number of desired groups in advance. We consider that this specification constitutes a form of semi-supervised learning. We performed k-means clustering using the *kmeans* function in R. k-means allows to group objects within a dataset based on centroid calculations, but requires a predefined number of clusters. Here, the number of clusters we test is set by relying on anatomical logic: clustering was performed for two groups (anterior and posterior teeth), three groups (premaxillary, maxillary, and dentary teeth), and six groups (premaxillary teeth, anterior maxillary teeth, posterior maxillary teeth, anterior dentary teeth, middle dentary teeth, and posterior dentary teeth). Finally, we performed unsupervised clustering analyses. This approach does not provide the algorithm with any a priori knowledge about cluster attribution and number. This approach was added in order to investigate the possibility of highlighting dental morphotypes from 3D GMM results alone. To run the unsupervised clustering analysis, we used the *mclust* function from the *mclust* R-package which calculates the most probable number of clusters in a dataset based on the detection of Gaussian

TABLE 1 Morpho-anatomical criteria employed in the comparative anatomy-based classification. In the "Operations" columns, "Y" indicates that the criterion is relevant and applied in the context of the operation. In the "Operator" columns, numbers denote the sequential order in which criteria were applied during the classification process; "n.u." indicates that the criterion was not used.

	Operations			Operators					
Morpho-anatomical criteria	Anatomical assignation relative to jawbone origin ([PM]; [M]; or [D])	Absolute positioning ([1–4]; [5–17]; [1–15])	Lateralization ([R] or [L])	RA	DA	JG	CLG	RP	RR-T
1-Crown wear facet location	Y	/	/	1	n. u.	3	4	4	3
2-Degree of crown symmetry/asymmetry	Y	Y	/	3	1	5	1	5	5
3-Lingual bulge	Y	/	/	5	n. u.	2	3	n. u.	4
4-General crown shape & crown width/length ratio	Y	Y	Y	4	2	1	2	3	6
5-Anterior projection of the mesial carina	Y	Y	/	6	3	6	5	6	7
6-Crown/root orientation	Y	/	/	n. u.	4	n. u.	n. u.	1	1
7-Convexity/concavity of the labial/lingual face	/	/	Y	2	n. u.	4	6	2	2
Total number of morpho-anatomical criteria used				6	4	6	6	6	7

distributions by maximum likelihood estimates and Bayesian criteria (Scrucca et al., 2023).

3 | RESULTS

3.1 | Comparative anatomy

3.1.1 | Classification criterion and operational sequence

Each operator spent approximately 7–8 h over 2 days to observe and classify all of the teeth based on his/her own determination. The operators used, independently and not necessarily in the same order, seven principal morphological features that we have standardized under the same terminology: (i) the location of wear facets on the crown (e.g., labially vs. lingually); (ii) the degree of crown symmetry/asymmetry; (iii) the presence or absence of a lingual bulge; (iv) the general shape of the crown (width to length ratio at maximal crown width); (v) the anterior projection of the mesial carina; (vi) the orientation of the crown in relation to the root; and (vii) the convexity/concavity of the labial/lingual surface (Figure 1a,b; Table 1). In the classification sequence, each operator initially determined the anatomical origin of the tooth by assigning it to a specific jawbone element (premaxilla [PM], maxilla [M], or dentary [D]). The other two operations (assigning an absolute position and determining lateralization) were carried out in different orders depending on the operator. Importantly, lateralization could only be assessed once the tooth had been attributed to a specific dental morphotype (i.e., premaxillary, maxillary, or dentary), as this step provides the necessary anatomical context for evaluating side-specific features. Indeed, once the teeth have been assigned to the upper or lower jaw, a combination of several characteristics observed in the teeth of turiasaurs makes it easy to determine their lateralization (Table 1) (Britt et al., 2017; Foster et al., 2026; Mateus et al., 2014; Milàn & Mateus, 2023; Mocho et al., 2016; Royo-Torres et al., 2006, 2017; Royo-Torres & Upchurch, 2012; Rozada et al., 2021; Sharma et al., 2022; Woodruff et al., 2025). Primarily, the teeth are convex labially and concave lingually. Additionally, the mesial carinae are always convex, while the distal carinae may show an apical concavity. The apex projection creates a concavity on this same carina and consequently orients the apex distally (Britt et al., 2017; Foster et al., 2026; Mateus et al., 2014; Milàn & Mateus, 2023; Mocho et al., 2016; Royo-Torres et al., 2006, 2017; Royo-Torres & Upchurch, 2012; Rozada et al., 2021; Sharma et al., 2022; Woodruff et al., 2025).

3.1.2 | Classification results

Among the 114 teeth examined, 68 (59.6%) were assigned to the same dental morphotype (PM, M, or D) by all operators (strict consensus); 30 were assigned to the same morphotype by at least 75% but fewer

than 100% of observations (weak consensus); and 12 were assigned by at least 60% but fewer than 75% of observations (weak conflict). Only four teeth remained in an absolute conflict with an equal (and highest) proportion of observations assigning them to two different morphotypes. Operator DA is involved in 48.7% of the total conflicting observations (weak consensus, weak conflict and absolute conflict, and in 80% of the conflicting observations resulting in weak consensus). The other operators were notably less involved in conflicting identifications, ranging from 6.4% to 15.4%. When DA's observations are excluded, the rate of strict consensus rises to 80.7%. This pattern is clearly reflected in the FAMD results (Data S3), where operator DA occupies a markedly distinct position from the other operators, who cluster more closely based on their classification of teeth into premaxillary, maxillary, and dentary morphotypes. Among the conflicting observations, 45.7% involved premaxillary and dentary teeth, and another 45.7% maxillary and dentary teeth. Conflicting observations between maxillary and premaxillary identifications were rare, accounting for only 4.3% of conflicting cases (Data S1).

Whether all observations or only strictly consensual ones are considered, the proportions of premaxillary, maxillary, and dentary teeth inferred from operator assignments are close to those expected under the assumption of a dentition similar to that of *Losillasaurus giganteus* (mean deviation from expected value = 8.3%; $\sigma = 4.1$). JG and RP both assigned the tooth reconstructed from the micro-CT scan of the left maxilla ANG12-1908 to the left maxillary position 7, which is fully consistent with its known identification. Overall, the identifications made by the six operators for the 114 teeth (plus the CT-scanned maxillary tooth) led to the establishment of a consensus regarding three distinct dental morphotypes: premaxillary, maxillary, and dentary.

Among the 114 teeth examined, only two were consistently assigned to the same morphotype and absolute position by all operators. The FAMD results indicate that the observers with the most similar locus determinations are RA, RP, and JG, who cluster closely in multivariate space (Data S3). Across the entire dataset, the mean range of positional variation—that is, the number of loci between the most divergent assignments—for a given tooth was 4.4 ± 2.3. When restricting the analysis to teeth for which a strict consensus was reached ($n = 68$), the mean positional deviation remained statistically equivalent at 4.3 ± 1.9. Including cases of weak consensus ($n = 30$) while excluding the conflicting assignments slightly reduced the average positional deviation to 3.9 ± 1.9 ($n = 98$). These results indicate that, on average, operators converge on an absolute position within approximately four loci for both upper jaw teeth (positions 1–17) and lower jaw teeth (positions 1–15).

This average precision in locus determination enables the broad identification of the previously arbitrary defined subcategories—anterior, middle, and posterior (see Materials and Methods). Among the 114 teeth examined, 43 (37.7%) were assigned by full consensus (100%) to one of these subcategories, and an additional 39 teeth (34.2%) were assigned to the same subcategory in a weak consensus (≥75% observations, but <100%).

3.1.3 | Description of tooth morphotypes

The following description of the premaxillary, maxillary, and dentary morphotypes is based on observations that have given rise to strict and weak consensus ($n = 98$). The teeth are all heart-shaped. Regarding general tooth shape, anterior teeth are much more symmetrical than posterior teeth due to a more convex mesial edge, while the distal edge is apically concave and basally convex (Figure 2). Only premaxillary teeth are almost symmetrical (Figure 2a,b). In the more mesial regions of the jaw, the apex of the teeth is aligned with the apicomesial axis of the crown base. In posterior teeth, the mesial carinae are strongly convex and project significantly mesially, causing the apex to re-orient distally. This asymmetry is a synapomorphy also present in other turiasaurs (Britt et al., 2017; Mocho et al., 2016; Royo-Torres et al., 2006; Royo-Torres & Upchurch, 2012; Saleiro & Tschopp, 2025) and sauropods such as *Europasaurus holgeri* (Régent et al., 2024). In contrast, anterior teeth have mesial carinae with minimal projection, also described in *Loillasaurus giganteus* (Royo-Torres et al., 2021). For the crown width to length ratio, dentary teeth have relatively more elongated crowns compared to the shorter, more robust crowns of premaxillary and maxillary teeth. Additionally, a bulge observed on the apical part of the lingual surface is a characteristic found exclusively in dentary teeth. There are no denticles on the teeth. The roots are cylindrical, with facets at regular intervals. In our case, it is difficult to determine whether there is a pattern to these facets.

In turiasaurs, the teeth of the upper jaw overlap those of the lower jaw, which implies surface contact between the lingual surface of upper teeth and the labial surface of lower teeth. Therefore, lingual wear facets are found on the upper teeth, while labial wear facets are present on the lower teeth. We also used this criterion to classify teeth based on their position in the upper and lower jaw (Régent et al., 2024). The orientation of the crown relative to the root is also useful criterion. In *Losillasaurus giganteus*, only the crowns of dentary teeth align with the root axis without ever intersecting it (Royo-Torres et al., 2021), which we also observed in some of our teeth preserving the root (Figure 1). In contrast, the premaxillary and maxillary crow axes intersect that of the root (Royo-Torres et al., 2021). Based on these morphological characters, each of the operators classified the teeth into three morphotypes, thus demonstrating at least qualitative heterodonty in Turisauria indet. from Angec-Charente.

This comparative anatomy method has proven highly effective, yielding very similar results. Among the 114 observed teeth, only 16 (14.0%) conflicts (weak conflict and strict conflict) arose when determining their morphotype. Thus, 86.0% of the identified teeth were consistently classified by all operators in a relatively short amount of time. However, when it comes to determining the precise locus of individual teeth, the results are significantly less reliable. The operators never reached the same conclusion regarding the exact locus of each tooth, except for two teeth (ANG23-9864 and ANG23-8165).

FIGURE 2 Selected representative isolated Turiasauria indet. teeth from Angeac-Charente, whose observation during comparative anatomy classification resulted in a consensual assignation to one of the three dental morphotypes (premaxillary, maxillary, dentary): a,b left premaxillary tooth (ANG16-4488; weak consensus) in labial (a) and lingual (b) views; c,d left anterior maxillary tooth (ANG13-2330; weak consensus) in labial (c) and lingual (d) views; e,f right posterior maxillary tooth (ANG18-6169; strict consensus) in labial (e) and lingual (f) views; g,h right anterior dentary tooth (ANG14-3129; strict consensus) in labial (g) and lingual (h) views; i,j right middle dentary tooth (ANG14-R267; strict consensus) in labial (i) and lingual (j) views; k–k, left posterior dentary tooth (ANG19-7173; weak consensus) in labial (k) and lingual (l) views. Scale bar a–l = 2 cm.

3.2 | 3D geometric morphometrics

The results of the PCA without complete crown (excluding the apex) are presented in Figures 3 and 4. The first three PCs account for 73% of the total variance. PC1, which explains 47.12% of the total variance, represents morphological variation related to the maximum curvature of the edge of the crown. Extremely positive shapes along PC1 correspond to teeth with the greatest crown width at the level of maximum curvature. Conversely, extremely negative shapes are characterized by teeth with a lower crown width at the same level (Figures 3 and 4). PC1 also highlights a stronger labial and lingual convexity in negative extremes when viewed distally. PC2, which explains 15.74% of the total variance, represents morphological variation related to the position of the maximum curvature point along the mesial edge of the tooth. The positive extreme along this component reflects a pronounced apical projection of the curvature point, giving teeth an asymmetrical appearance mesio-distally. In contrast, the negative extreme corresponds to shapes where the mesial curvature point aligns with the distal one, resulting in a more symmetrical tooth shape mesio-distally (Figures 3 and 4).

In the scatterplot, it is evident that the two qualitatively determined tooth types (premaxillary and maxillary) are distinctly

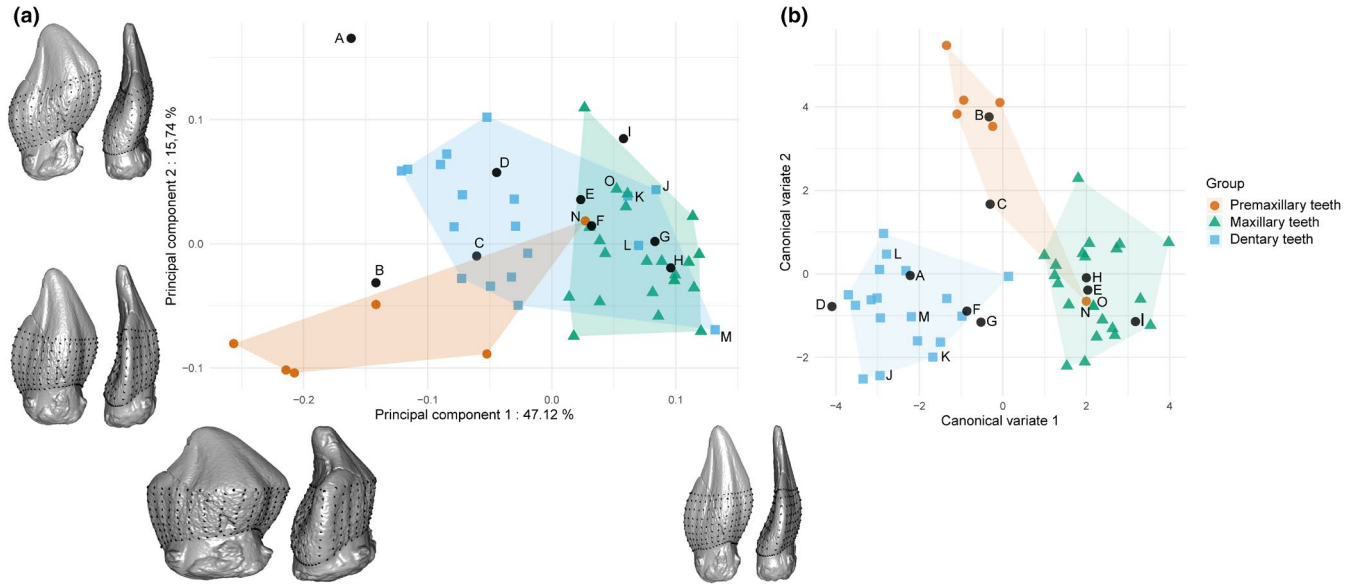

FIGURE 3 Tooth shape variation of Turiasauria indet. from Angeac-Charente (without complete crown dataset—apex not included) based on three dental categories (premaxillary, maxillary, and dentary teeth). (a) Graphical representation of the two first principal components (PCs) from the PCA, which together account for 62.86% of the total variance. Tooth morphologies and their corresponding landmark configurations are shown in labial and distal views at the extremes of each PC axis. (b): Graphical representation of the two first canonical variates from corresponding CVA. In both A and B, each data point represents a single isolated tooth. Points A–I correspond to conflictual teeth, while points J–O represent identified teeth that occupy unexpected positions in morphospace.

separated (Figure 3a). However, the morphological space occupied by dentary teeth overlaps with that of the other types, particularly due to the presence of peculiar dentary teeth within the maxillary group, labeled point J to M (Figure 3a; ANG14-R288 (J), ANG17-R2109b (K), ANG19-7170 (L), and ANG14-R267 (M)). This result is congruent with the results of anatomical comparisons, which reveal maximum conflict between dentary and maxillary/premaxillary teeth. It is also consistent with an intermediate position of dentary teeth between premaxillary and maxillary teeth within the morphological space. When observing the associated CVA plot (Figure 3a), the overlap between clusters is significantly reduced. This separation is supported by the k-NN analyses conducted for the three morphotypes (Table 2). Indeed, k-NNs achieve 77.78% correct reassignment. The presence of point N (ANG14-R435), a tooth identified by all operators as premaxillary, is located far from the other premaxillary teeth and where the maxillary and dentary teeth overlap within the morphological space. Points labeled A to I (Data S4) correspond to teeth for which qualitative identification is conflictual among operators. Using 3D GMM, they have been a posteriori assigned to groups consistent. The tooth ANG19-7172 (A) is notably isolated from the main cluster. Despite this, the tooth exhibit extreme wear facet. Its extreme placement along PC2 is explained by a pronounced projection of the mesial carina and its wear facet.

In the same morphological space, we further subdivided the morphotypes based on their position in the jaw (anterior and posterior maxillary teeth, anterior and posterior dentary teeth, and premaxillary teeth) (Figure 4a). It can be observed that the clusters corresponding to anterior teeth are slightly more negative along PC2 relative to more posterior teeth for both maxillary and dentary groups and that the most posterior teeth exhibit significantly greater asymmetry along this PC in mesio-distal view. Nonetheless, there is significant overlap between the anterior and posterior groups of both dentary and maxillary teeth. For these five tooth morphotypes, although the point clouds of anterior and posterior maxillary teeth, as well as those of anterior and posterior dentary teeth, show some overlap, they remain distinct according to k-NN results with only 57.40% correct reassignment (Table 3). The observed overlaps in the scatterplot are likely due to the subjective nature of defining anterior and posterior positions in the jaw. The mesio-distal shape variations within the same main dental morphotype (premaxillary, maxillary, and dentary) are subtle and relate more to a variation in size than in shape. k-NN was also conducted on the separation between anterior and posterior teeth only. Although this division is arbitrarily defined by operators, it is nonetheless supported by k-NN results of 66.67% accuracy (Table 4).

PC3 accounts for 10.63% of the total variance and is related to shape variation of the cervix (Figure 4b). Data points with the most positive values correspond to teeth with a significantly more asymmetrical cervix compared to those with the most negative values. Shape variation along this component is also related to variation of the mesiodistal length of the teeth, with longer positive teeth mesiodistally than negative teeth. The morphological spaces occupied by the three qualitatively determined tooth types show minimal overlap on this axis. Point O, corresponding to segmented maxillary tooth 7, is notably isolated from other maxillary teeth. As with PC1 and PC2, there is no clear separation between anterior and posterior teeth, whether maxillary or dentary, along PC3.

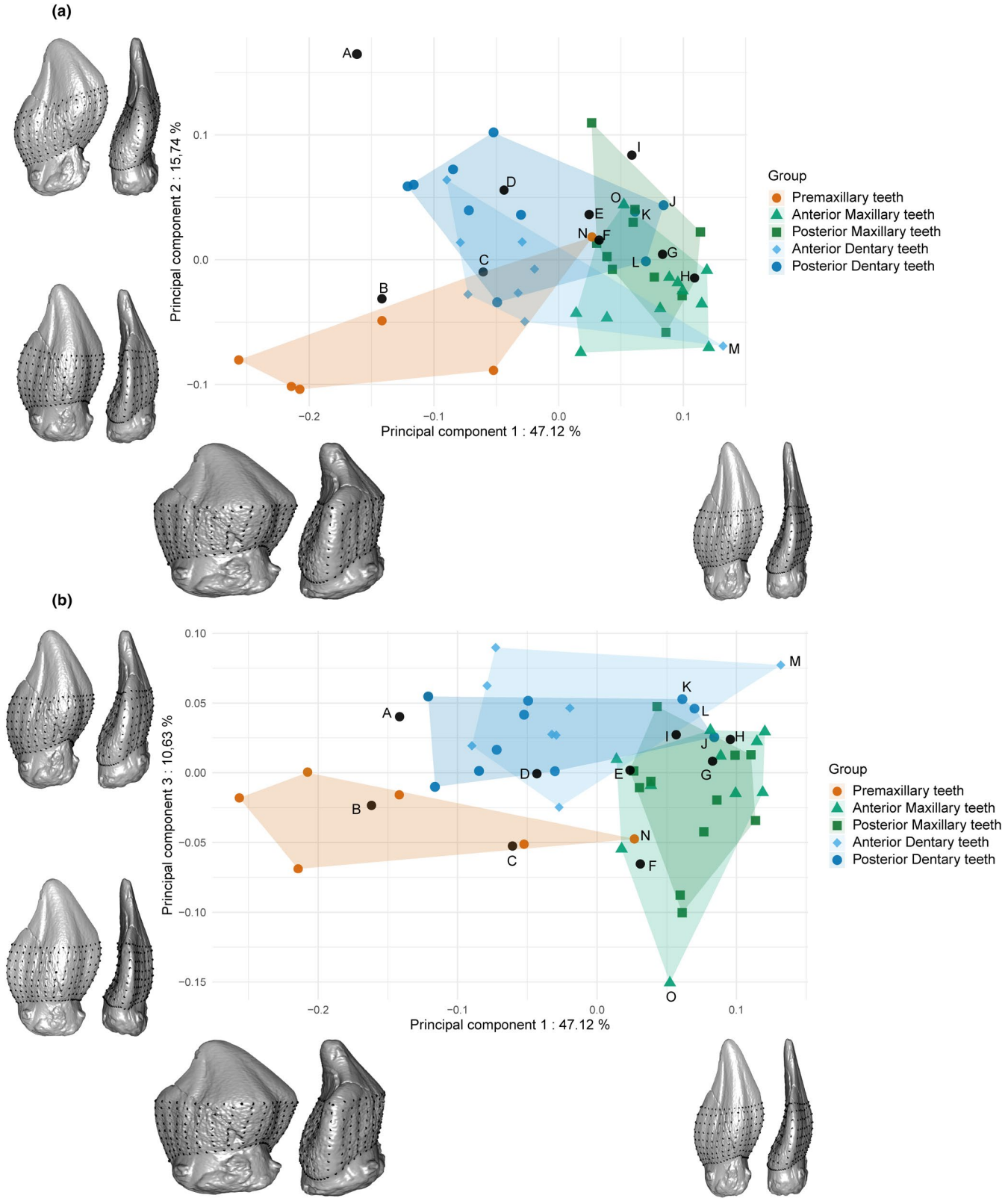

FIGURE 4 Tooth shape variation of Turiasauria indet. from Angeac-Charente (without complete crown dataset—apex not included—same morphospace as Figure 3) based on five dental categories (premaxillary, maxillary anterior, maxillary posterior, dentary anterior, and dentary posterior teeth). (a) Graphical representation of the two first principal components (PCs) from the PCA, which together account for 62.86% of the shape variation. Tooth morphologies and their corresponding landmark configurations are shown in labial and distal views at the extremes of each PC axis. Each data point represents a single isolated tooth. Points A–I correspond to conflictual teeth, while points J–O represent identified teeth that occupy unexpected positions in morphospace. (b) Graphical representation of the first and third PCs, which together account for 57.75% of the total variance.

To determine whether tooth size influences the classification of turiasaurian teeth, MANOVAs were performed on centroid size variation. Pairwise comparisons were conducted for the three qualitatively determined tooth morphotypes (premaxillary, maxillary, and dentary) as well as for the anterior (anterior maxillary and anterior dentary) and posterior (posterior maxillary and posterior dentary) positions of the teeth. The MANOVAs reveal a significant difference among the three groups, premaxillary, maxillary, and dentary (p-value <0.05), but when comparing groups pairwise, we can see no significant difference between maxillary and premaxillary teeth. For the five groups (premaxillary, anterior and posterior maxillary, anterior and posterior dentary), there is a significant difference between the different groups (p-value <0.01) (Figure 5a). More specifically, size differences are significant between premaxillary teeth and posterior maxillary and dentary teeth. The size of anterior maxillary teeth is different from anterior and posterior dentary teeth and posterior maxillary teeth (Figure 5a). Lastly, the size of anterior teeth is significantly different from posterior teeth (p-value <0.01).

The same analyses were conducted on the 20 3D surface models of complete teeth with an apex free of wear facets, which could alter their overall shape. PC1, explaining 52.96% of the total variance, represents the distribution of specimens based on the shape of the apex (Figure 6a). The positive extreme along this PC is characterized by an apex that is highly projected toward the distal edge of the tooth. On the positive side of PC1, this apex is very small, compact, and positioned closer to the points of maximum curvature of the ridges. These teeth are highly asymmetrical mesiodistally and display pronounced lingual concavity. Conversely, the negative extreme of PC1 represents a much more symmetrical tooth mesiodistally with a larger apex oriented upward. Additionally, the lingual concavity is significantly reduced. The second component, which explains 22.28% of the total variance, represents the apico-mesial projection of the mesial ridge in extreme shapes (Figure 6a). Teeth with the most negative values along PC2 exhibit a more symmetrical crown mesiodistally compared to those with the most positive values. Furthermore, the lingual convexity is more pronounced in the extreme positive shapes of this component than in the negative extremes.

In this PCA, when considering PC1 and PC2, the morphological spaces occupied by the three qualitatively determined tooth types are completely isolated from one another, with no overlap (Figure 6a). This lack of overlap persists even when considering not three, but five qualitative morphotypes (anterior and posterior maxillary teeth, anterior and posterior dentary teeth, and premaxillary teeth) (Figure 6a). This separation is strongly supported statistically by the CVA analyses conducted for the three morphotypes, with a result of 100% correct reassignment into the predefined groups (Table 5). k-NN results show 85% correct reassignment (Table 6). For the five dental morphotypes, although the clusters of anterior and posterior maxillary teeth, as well as those of anterior and posterior dentary teeth exhibit some overlap, they remain distinct as previously observed, with 65% correct reassignment using k-NNs (Table 7). The same tests were also performed by separating only the anterior and posterior teeth. This separation is justified, with a k-NN result of 80% (Table 8). Additionally, posterior teeth, whether maxillary or dentary, are predominantly distributed along the most positive regions of the PCAs' graphs.

The third component accounts for 6.14% of the total variance and represents the labial asymmetry of the tooth cervix. Along this component, teeth with the most positive values exhibit greater concavity on the lingual surface compared to those with the most negative values. It is also evident that anterior teeth are represented by more positive points on the axis of the third component than posterior teeth (Figure 6b). A notable overlap is observed between anterior and posterior dentary teeth, whereas no overlap exists between anterior and posterior maxillary teeth. Additionally, points F and G, corresponding to teeth with previously indeterminate placement, remain identifiable along this component (Figure 6b).

TABLE 2 Results of k-NN analyses for the three groups of teeth (premaxillary teeth, maxillary teeth, dentary teeth) for the dataset without complete crown (excluding the apex; n = absolute values), considering 95% of the variance.

	Comparative anatomy classification		
k-NN classification	Premaxillary teeth	Maxillary teeth	Dentary teeth
Premaxillary teeth	4	0	2
Maxillary teeth	1	23	3
Dentary teeth	2	4	15

TABLE 3 Results of k-NN analyses for the five groups of teeth (premaxillary teeth, anterior maxillary teeth, posterior maxillary teeth, anterior dentary teeth, posterior dentary teeth) for the dataset without complete crown (excluding the apex; n = absolute values), considering 95% of the variance.

	Comparative anatomy classification				
k-NN classification	Premaxillary teeth	Anterior maxillary teeth	Posterior maxillary teeth	Anterior dentary teeth	Posterior dentary teeth
Premaxillary teeth	4	0	0	1	1
Anterior Maxillary teeth	1	7	3	1	2
Posterior Maxillary teeth	0	4	9	0	0
Anterior Dentary teeth	0	0	0	5	2
Posterior Dentary teeth	2	2	2	2	6

Regarding analyses including tooth apices, MANOVAs highlight a significant difference (p-value <0.01) among the three groups (premaxillary, maxillary, and dentary). The only non-significant size difference is between maxillary and dentary teeth. For the five morphotypes, as observed previously, sizes are significantly different (p-value <0.01) between anterior maxillary teeth, posterior maxillary teeth, anterior and posterior dentary teeth, as well as between premaxillary teeth, anterior and posterior dentary teeth and posterior maxillary teeth (Figure 5b). The size difference remains significant between anterior and posterior teeth (p-value <0.01). These analyses suggest that tooth size significantly influences classification and position, but that the continuity of the dental row must be taken into account.

TABLE 4 Results of k-NN analyses for the two groups of teeth (anterior and posterior) for the dataset without complete crown (excluding the apex; n = absolute values), considering 95% of the variance.

	Comparative anatomy classification	
k-NN classification	**Anterior**	**Posterior**
Anterior	19	8
Posterior	10	17

3.3 | Classification

3.3.1 | Supervised classification: k-NN

To determine whether it is possible to identify the positions of conflicting teeth using a supervised algorithm, predictions made by the best k-NN retained after cross-validation allow for the classification of conflicting teeth based on a training dataset. The classifications of teeth considered as absolute conflict show no difference between

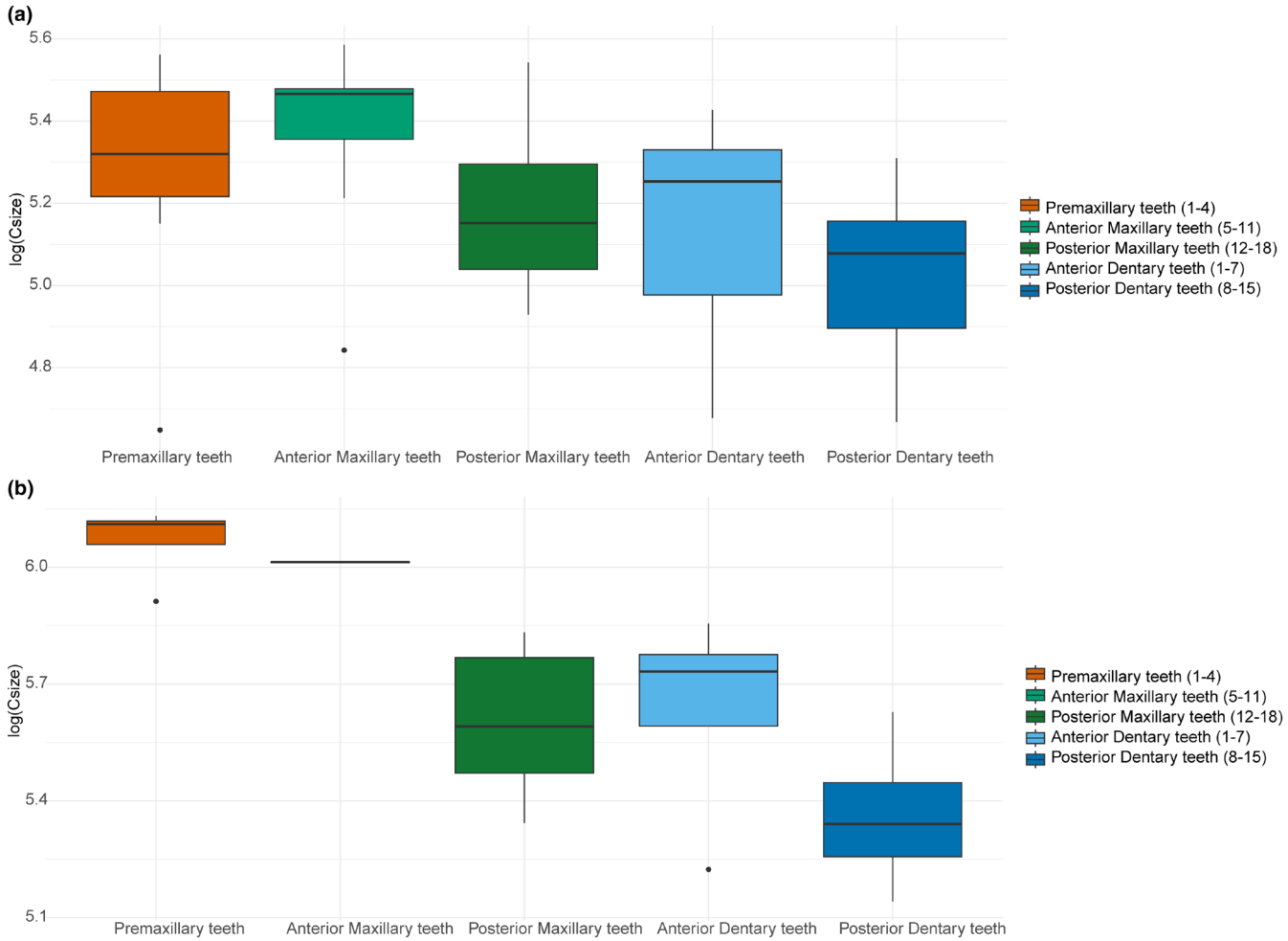

FIGURE 5 (a) Statistical comparison of the different dental categories obtained from comparative anatomy determination of the Turiasauria indet. teeth from Angeac-Charente (without complete crown dataset—apex not included), following MANOVA analysis. X-axis represents the morphological dental categories: Premaxillary, anterior maxillary, posterior maxillary, anterior dentary, and posterior dentary teeth. Y-axis represents the centroid size (Csize). The MANOVA analysis reveals a significant difference among the five groups, with a p-value of 0.00335. (b) Comparison of the dental morphological groups of the turiasaurian sauropod teeth from Angeac-Charente, including the tooth apex, following MANOVA analysis. The MANOVA analysis reveals a significant difference among the five groups, with a p-value of 0.00112.

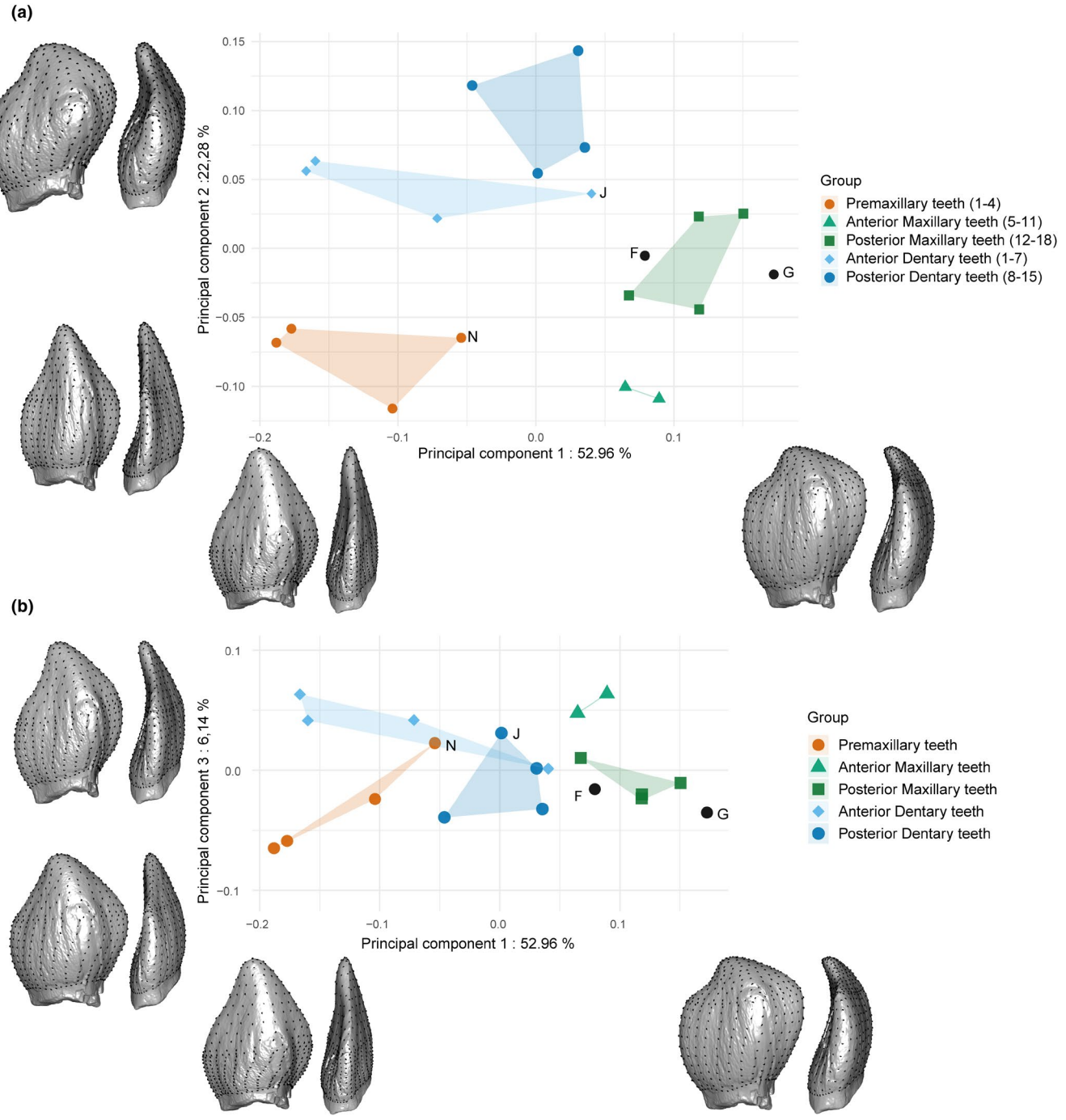

FIGURE 6 Tooth shape variation of Turiasauria indet. from Angeac-Charente (with complete crown dataset—apex included) based on five dental categories (premaxillary, anterior maxillary, posterior maxillary, anterior dentary, posterior dentary). (a) Graphical representation of the two first principal components (PCs) from the PCA, which together account for 75.24% of the total variance. Tooth morphologies and their corresponding landmark configurations are shown in labial and distal views at the extremes of each PC axis. Each data point represents a single isolated tooth. Points F and G correspond to conflictual teeth, while points J and N represent identified teeth that occupy unexpected positions in morphospace. (b) Graphical representation of the first and third PCs, which together account for 59.10% of the total variance.

the k-NNs prediction algorithm and human assessment. When identifying premaxillary, maxillary and dental teeth, regardless of whether the apex is taken into account or not, the correct determination rate is 100%. Furthermore, for the same dataset excluding the apex, when determining conflicting teeth based on their anteroposterior position, only one tooth is not classified in accordance with the operators. Specifically, tooth B (ANG17R-1723) is classified as an anterior dentary tooth by k-NN, whereas the operators identify it as a premaxillary tooth. When considering five groups (premaxillary teeth, anterior maxillary teeth, posterior maxillary teeth, anterior dentary teeth, and

posterior dentary teeth), the predictions match the determinations of the operators in 55.5% of cases regarding locus position.

Three other teeth exhibit discrepancies between comparative anatomy and supervised classification. These differences are not related to bone position but rather to anteroposterior positioning. Specifically, teeth A (ANG19-7172) and C (ANG11-918) are classified as posterior dentary teeth by the operators but as anterior dentary teeth by the algorithm. Additionally, tooth G (ANG15R-639) is identified as an anterior maxillary tooth by the algorithm, whereas the operators classify it as a posterior maxillary tooth.

3.3.2 | Semi-supervised classification

We also performed semi-supervised k-means clustering on PC1 and PC2, specifying 2, 3, 5, and 6 groups. Clustering with two and six groups revealed no biologically significant patterns in our material. The aim of this grouping was to determine whether it could distinguish left teeth from right or separate anterior and posterior teeth. For the semi-supervised clustering with three groups, the resulting clusters appear more coherent. In the dataset without apex, the groups closely align with those we defined by comparative anatomy (premaxillary teeth, maxillary teeth, and dentary teeth). In fact, 49 of 54 teeth are classified in the same groups as the operators, giving 90.74% of teeth placed in the same group by the algorithm and the operators. This also works well for the apex dataset, with 17 of 20 teeth (i.e., 85% of teeth), having identical determinations between the algorithm and the operators. For the clustering analysis with five groups, the goal was to determine whether we could recover the predefined categories premaxillary teeth, anterior maxillary teeth, posterior maxillary teeth, anterior dentary teeth, and posterior dentary teeth. Results are poorer than described above. Indeed, 35 teeth of 54 (i.e., 64.81% of teeth) have identical determinations between the algorithm and the operators. For the dataset with apex, the clustering analysis revealed no biologically sensical groups for six groups requested.

TABLE 5 Results of CVAs analyses including 95% of the variance for the three groups of teeth (premaxillary teeth, maxillary teeth, dentary teeth) for the dataset with complete crown (excluding the apex; *n* = absolute values) (Kappa statistic = 1).

	Comparative anatomy classification		
CVA classification	Premaxillary teeth	Maxillary teeth	Dentary teeth
Premaxillary teeth	4	0	0
Maxillary teeth	0	8	0
Dentary teeth	0	0	8

TABLE 6 Results of k-NN analyses for the three groups of teeth (premaxillary teeth, maxillary teeth, dentary teeth) for the complete crown dataset (*n* = absolute values), considering 95% of the variance.

	Comparative anatomy classification		
k-NN classification	Premaxillary teeth	Maxillary teeth	Dentary teeth
Premaxillary teeth	3	0	0
Maxillary teeth	0	7	1
Dentary teeth	1	1	7

3.3.3 | Unsupervised classification

Unsupervised clustering performed on all PCs with the variable equal identification (VEI) model selected by the Bayesian information criterion (BIC) fails to produce different anatomical groups defined a priori by operators with our different datasets. Indeed, it yields either a single cluster or nine clusters without any group pattern. Furthermore, the highest uncertainty for specimen cluster assignment is 44.5%. In other words, the algorithm only manages to assign a cluster to a tooth to the extent of 55.5%.

4 | DISCUSSION

4.1 | Comparative anatomy classification

Although each operator was free to develop their own classification protocol, seven morpho-anatomical criteria were consistently and nearly systematically applied by all of them (Table 1). Differences

TABLE 7 Results of k-NN analyses for the five groups of teeth (premaxillary teeth, anterior maxillary teeth, posterior maxillary teeth, anterior dentary teeth, posterior dentary teeth) for the complete crown dataset (*n* = absolute values), considering 95% of the variance.

	Comparative anatomy classification				
k-NN classification	Premaxillary teeth	Anterior maxillary teeth	Posterior maxillary teeth	Anterior dentary teeth	Posterior dentary teeth
Premaxillary teeth	3	0	0	0	0
Anterior Maxillary teeth	0	2	0	0	0
Posterior Maxillary teeth	0	0	5	0	1
Anterior Dentary teeth	1	0	0	2	2
Posterior Dentary teeth	0	0	1	2	1

TABLE 8 Results of k-NN analyses for the two groups of teeth (anterior and posterior) for the complete crown dataset (*n* = absolute values), considering 95% of the variance.

	Comparative anatomy classification	
k-NN classification	**Anterior**	**Posterior**
Anterior	8	2
Posterior	2	8

in classification arise from the fact that these criteria were not prioritized in the same way and that some of them were disregarded by certain operators (Table 1). In this regard, it is noteworthy that operator DA did not consider the morpho-anatomical criterion of crown wear facet location (Table 1) despite its potential importance in preventing conflicting interpretations between premaxillary and dentary teeth, as well as between maxillary and dentary teeth. This criterion is particularly relevant given that the lingual surface of upper teeth overlaps the labial surface of lower teeth (Royo-Torres et al., 2021; Wiersma & Sander, 2016), resulting in wear facets primarily on the lingual and labial sides, respectively. This pattern is also found in *Losillasaurus giganteus* (Royo-Torres et al., 2021), *Camarasaurus lentus* (Wiersma & Sander, 2016), and *Europasaurus holgeri* (Régent et al., 2024). This single methodological difference results in a different classification of teeth, particularly between premaxillary and anterior dentary teeth. These teeth, being highly similar due to their anterior positioning (Royo-Torres et al., 2021), are sometimes distinguished by the presence of wear facets and the lingual bulge for the dentary teeth. This bulge is also present in *Losillasaurus giganteus* (but not described by the authors: Royo-Torres et al., 2021). This feature serves as a critical distinguishing factor between dentary teeth and other types of teeth. Without considering this feature, upper and lower teeth may be misidentified and assigned incorrect positions—precisely what occurred with this operator.

To assign teeth an absolute position, the general shape and size of the tooth is often the first criterion considered. Indeed, this characteristic is relevant for determining their relative anteroposterior position in the jaw. In certain sauropods, the larger teeth are more anterior than the smaller posterior teeth. This is true for the heart-shaped teeth of turiasaurs such as *Losillasaurus giganteus* (Royo-Torres et al., 2021) as well as for the spatula- and compressed cone-chisel-shaped teeth of basal Macronaria such as *Camarasaurus* (Wiersma & Sander, 2016) and Brachiosauridae (Mannion et al., 2017). However, it is important to note that ontogeny may overlap with this criterion of relative positioning based on size, which is why the general shape of the tooth must also be taken into account. Thus, two teeth that have a similar general shape but markedly different sizes most likely belonged to individuals at different ontogenetic stages. For instance, two small teeth (ANG13-R187; ANG22-7891) were thus identified as middle or anterior dentary teeth of a juvenile specimen by all operators. To distinguish anterior from posterior teeth, the symmetry of the tooth, the projection of the mesial carina, and the general size of the tooth are considered.

First, with this methodology, it is possible to classify the teeth into several groups by organizing the determination criteria. The four most general traits which allow us to group teeth are the general shape of the crown, proxied by the crown length/width ratio, the presence or absence of the lingual bulge, the projection of the mesial carina, and the orientation of the crown in relation to the root. These criteria appear to be typical of turiasaurian teeth and highlight the separation between upper and lower jaw teeth, as well as between right and left. Subsequently, other traits are used to refine the classification. For teeth where uncertainty about their upper or lower jaw position persists, additional criteria such as crown orientation, lingual bulge, and wear facets are applied. Lateralization can only be defined after the operation of morphotype assignments and is easily solved thanks to morphological criteria such as the convexity and concavity of the labial and lingual surfaces (Table 1). The teeth asymmetry is closely associated with the anterior projection of the mesial carinae as observed in the premaxillary teeth of other sauropods/turiasaurs (Moore et al., 2018; Régent et al., 2024; Royo-Torres et al., 2021). When attempting to reposition teeth within a jaw using comparative anatomy, it is therefore necessary to be familiar with and be able to identify on specimens the diagnostic features specific to each group and to the morphological position within the jaw. This method is entirely applicable to other groups such as theropods or crocodilians, in which numerous isolated teeth as well as teeth in situ are known, allowing for comparison (Alonso et al., 2018; Averianov et al., 2019; D'Amore et al., 2019; Fanti & Therrien, 2007; Rozada et al., 2021).

During the observation process, operators exhibited occasional hesitation regarding the most accurate placement on the jaw bones. These uncertainties could stem from a lack of distinguishing characteristics or excessive morphological similarity. Eight conflicts between operators were observed in distinguishing whether a tooth was inserted in the dentary or premaxilla, while 11 conflicts involved distinguishing between the dentary and maxilla. All operators followed a largely similar classification approach. Indeed, the prioritization of their identification criteria appears relatively consistent, following a pattern from broader to more specific anatomical features, as previously described. Moreover, tooth size generally decreases along the anteroposterior axis of the jaw (Mannion et al., 2017; Royo-Torres et al., 2021; Wiersma & Sander, 2016). Consequently and depending upon our a priori knowledge of the tooth morphology of *Losillasaurus giganteus* (Royo-Torres et al., 2021), comparative anatomy alone cannot accurately determine the exact location of teeth in the jaw of the Angeac-Charente turiasaure, hence the implementation of a methodology incorporating other approaches.

4.2 | 3D geometric morphometrics

The PCAs clearly highlight a distinction between premaxillary, maxillary, and dentary teeth when the apex can be analyzed (absence of wear facets, complete crown dataset) (Figure 6). However, overlaps are observed when the apex is not included (without complete

crown dataset) (Figures 3 and 4), which can be attributed to morphological continuity despite the differences in the positional placement of the teeth within the jaws (Chatterjee & Zheng, 2002).

Like in *Losillasaurus giganteus* (Royo-Torres et al., 2021), premaxillary teeth are the most distinct from the others. These teeth are markedly different due to their greater symmetry compared to maxillary and dentary teeth. They have a very slight concavity compared to the other teeth, indicating a wider apex. Additionally, the mesial projection of the apex is minimal or absent, and the cervix is straight. This third component reveals that dentary teeth tend to have a less straight and more curved cervix than maxillary teeth. The strict separation of morphotypes when the apex is considered underscores the importance of apex projection and orientation in distinguishing between dentary and maxillary teeth (Ribeiro Relvas, 2023). This justifies the use of discriminating features such as general crown shape, lingual bulge, and anterior projection of the mesial carina (Table 1) in comparative anatomy. These characteristics are also found in other sauropods with spatulate teeth, such as *Camarasaurus* (Ribeiro Relvas, 2023; Wiersma & Sander, 2016). In *Camarasaurus*, crown height also decreases significantly in the distal region of the jaw, and premaxillary teeth are very large with an upward-oriented apex (Ribeiro Relvas, 2023; Wiersma & Sander, 2016). The separation between anterior and posterior teeth (dataset with complete crown) occurs along the second component (Figure 6a), further highlighting the correlation between crown height and distal apex projection, as previously noted in *Losillasaurus giganteus* and *Camarasaurus* (Royo-Torres et al., 2021; Wiersma & Sander, 2016). The anteroposterior continuity of teeth within the jaw demonstrates a size gradient from largest to smallest along the second component, as well as a gradient in apex projection, transitioning from more symmetrical to less symmetrical shapes mesiodistally, as shown by the extreme shapes on the PCA (Figures 3 and 6a).

4.3 | Quantitative vs. qualitative observations

Among the 20 teeth with qualitative determination conflicts (weak and absolute) (Data S1), only nine well-preserved teeth were included in the quantitative analysis (ANG19-7172 (A), ANG17-R1723 (B), ANG11-918 (C), ANG11-837 (D), ANG14-3052 (E), ANG21-7384 (F), ANG15-R639 (G), ANG14-2964 (H), ANG14-R349 (I)) (Figure 7). To resolve these operators' identification conflicts, we considered the distribution of specimens across the PCA morphospace (validated by CVA and k-NNs; Tables 3 and 7), the results of the predicted classifications made by k-NNs as well as a finer re-examination of fine tooth anatomy.

Four teeth can be re-identified as posterior dentary teeth. The tooth ANG19-7172 (Figure 7a) stands out as an outlier, explained by a taphonomical impact on the distal carina, which is only visible through comparative anatomy. Based on PC1 and supervised

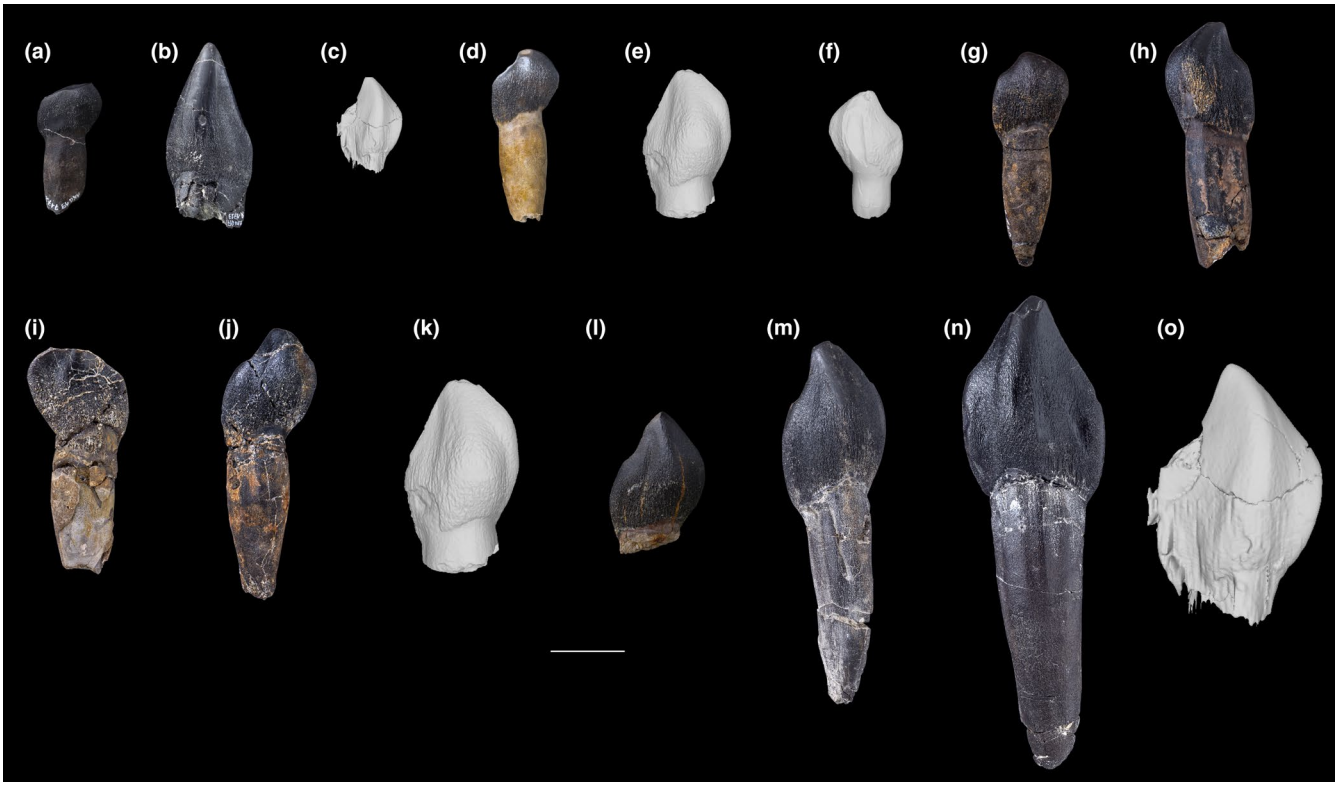

FIGURE 7 Representation of teeth of sauropod turiasauria indet. from Angeac-Charente with conflicting descriptions among operators and with a new description thanks to comparative anatomy, GMM, and clustering in labial view: ANG19-7172 (a); ANG17R-1723 (b); ANG11-918 (c); ANG11-837 (d); ANG14-3052 (e); ANG21-7384 (f); ANG15R-639 (g); ANG14-2964 (h); ANG14-R349 (i); ANG14R-288 (j); ANG17R-2109b (k); ANG19-7170 (l); ANG14R-267 (m); ANG14-435 (n); segmented maxillary tooth (o). Scale bar A–O = 2 cm.

classification, it appears to be a posterior dentary tooth (Figure 3a). The tooth ANG11-918 (Figure 7c) is positioned between premaxillary and dentary teeth in the PCA and is classified as maxillary by some operators due to its wear facets. Its asymmetry is too pronounced and its SI is significantly lower than that of premaxillary teeth. These results, combined with k-NN predictions as well as its small size, place it as a posterior dentary tooth. The same applies to the tooth ANG11-837 (Figure 7d): all PCA axes, supervised classification results, and wear facets classify it as a posterior dentary tooth. Finally, tooth ANG14-3052 (Figure 7e), which lies at the boundary between the morphological spaces of the dentary and maxillary teeth in the PCA, can be identified as a posterior dentary tooth thanks to the orientation of the crown axis relative to the root and the results of the supervised classification.

The following three teeth are also posterior teeth, but they belong to the maxillary category. The teeth ANG21-7384 (Figure 7f) and ANG15R-639 (Figure 7g) are clearly positioned within the maxillary cluster in the PCA (Figure 6), and both classification analysis and crown/root orientation confirm this assignment. Finally, the tooth ANG14R-349 (Figure 7i) is taphonomically damaged with numerous cracks and fractures. While most operators identify it as a dentary tooth, supervised classification and its distribution on the PCA morphospace allow us to position it as a posterior maxillary tooth. General crown shape and size, crown/root orientation, and the presence of a possible lingual bulge, all unambiguously, suggest a dentary tooth; however, to maintain consistency with the quantitative analyses, we choose to be classified it as a posterior maxillary tooth.

The tooth ANG17R-1723 (Figure 7b) is placed among dentary or premaxillary teeth by operators. Its pronounced symmetry, PCA results, and k-NN predictions lead to its identification as a premaxillary tooth. The tooth ANG14-2963 (Figure 7h) is unanimously recognized as maxillary, but its exact placement remains uncertain. It is classified either as an anterior or a posterior tooth. Its position in the morphological space resulting from PCA is not conclusive, while supervised classification favors an anterior placement. Given its size between the largest and smallest teeth, it is therefore classified as intermediate.

Four teeth (ANG14-R288 (J), ANG17-R2109b (K), ANG19-7170 (L), and ANG14-R267 (M) (Figure 7j,m)) are noteworthy. All of them were identified, without conflict, as anterior or middle dentary teeth using the qualitative method, but they occupy unexpected positions in certain morphological spaces (Figure 3a). On the first two components of the PCA without the apex (Figure 3), they appear highly positive on PC1 and fall within the maxillary teeth cluster. They have a relatively larger crown without having a different SI than the other dentary teeth. Along PC3, the four teeth are located within the dentary tooth cluster but remain at the limit of the maxillary one (Figure 4b). When examining the statistical results, CVAs indicate a significant separation between groups, and in the graphical representation, these teeth fall within the morphological space of dentary teeth. Despite their eccentric positions in the PCA, they remain consistent with the dentary tooth group.

The tooth ANG14-R435 (N) (Figure 7) was qualitatively identified as a premaxillary tooth; however, in the PCA, it appears highly displaced from the rest of the premaxillary group. This is likely due to its slight mesiodistal asymmetry and a very high maximum curvature on its crown. Given its placement at the intersection of the three groups in morphological space, its classification remains uncertain. It nevertheless closely resembles a maxillary tooth, with pronounced wear facets that significantly alter its shape, so with the support of our CVAs, we consider it to be a very anterior maxillary tooth. It is worth noting that this tooth was previously figured in Allain et al. (2022), who proposed it to be a left dentary tooth.

Whereas we would have expected the segmented replacement maxillary tooth (O) (Figure 7o) to be recovered as an outlier because of an unusual degree of labio-lingual compression, it falls perfectly within the maxillary tooth cluster. This provides a reliable reference tooth with a confirmed identification, as it was found in situ in the third alveolus of the maxillary bone. The placement of this tooth in the analyses reinforces the results of this study and justifies their use in guiding future investigations.

4.4 | Influence of size

The conduction of MANOVAs revealed a significant size difference among the various dental morphotypes based on quantitative determination (Figure 5). For the dataset with and without complete crown, a significant size difference was observed between anterior and posterior teeth. Smaller teeth appear to be significantly positioned more distally in the jaw compared to larger teeth. This finding supports the use of this characteristic to position teeth. Additionally, a significant size difference exists between premaxillary and dentary teeth, as well as between dentary and maxillary teeth. In contrast, no significant size difference was detected between premaxillary and anterior maxillary teeth nor between premaxillary and anterior dentary teeth. This is likely attributable to the continuity of these teeth in the upper jaw (Chatterjee & Zheng, 2002) and the anterior positioning of premaxillary and anterior dentary teeth in the dentary row. Crown height and consequently overall tooth size thus influence their placement within the jaw and should be considered during identification, as anterior teeth are larger than posterior teeth.

4.5 | Classification methods

The teeth identified differently by the operators and the machine are the ones that are positioned relatively close to each other in the jaw. Specifically, the discrepancies occur between the anterior and posterior dentary teeth or between the premaxillary and anterior dentary teeth. However, when the apex is taken into account, there is a 100% match between the determination of the operators and k-NN predictions. Therefore, there is little difference between comparative anatomy analysis and the classification method used here. This approach has proven to be consistently effective, as seen in

the analysis of certain diseases (Rajathi & Radhamani, 2016), with relatively high success rates (Goyal, 2022). The supervised clustering stays depending on the comparative anatomy carried out beforehand.

The identification of all teeth is less effective when using semi-supervised and unsupervised classifications. Indeed, automatic clustering fails to highlight meaningful groups or forms biologically incoherent clusters. Semi-supervised clustering, on the other hand, yields better results than fully automatic clustering. Specifically, for the three dental groups, 90.74% of determinations match those of the operators without considering the apex, while this rate drops to 64.8% when the apex is included. This drop is undoubtedly caused by the small number of teeth taking into account the apex, which means that the algorithm cannot train on a large number of teeth. For five groups, 64.8% of determinations align with the operators for the dataset without the apex, but the method fails entirely when the apex is included. Better results, which can enhance classification accuracy (Anderson et al., 2012), are obtained when the algorithm is provided with a predefined number of clusters. This trend is also observed in other fields, such as genetics, where clustering algorithms like tight-clustering and model-based clustering consistently outperform other clustering methods on both simulated and real data (Thalamuthu et al., 2006).

4.6 | Comparison of methods

Only one previous study has combined comparative anatomy, geometric morphometrics, and classification methods, and this was in order to analyze the isolated teeth of theropod dinosaurs (Hendrickx et al., 2023). In light of our study, we can now conclude that, in general, dental morphology provides sufficient criteria to distinguish premaxillary, maxillary, and dentary teeth in sauropods via different classification approaches (Chatterjee & Zheng, 2002; Mocho et al., 2016; Régent et al., 2024; Royo-Torres et al., 2021; Wiersma & Sander, 2016). To precisely differentiate between anterior and posterior teeth within the maxillary and dental morphotypes, tooth size must nevertheless be considered and compared. This finding suggests that to go beyond 3D GMM—which does not account for size variation—it is essential to integrate tooth size into the classification process to achieve a biologically accurate representation of dental arrangement within the jaw. The use of a combined approach involving comparative anatomy, 3D geometric morphometrics, and classification thus constitutes a comprehensive method that yields the most complete results possible.

We have demonstrated that the comparative anatomy is highly effective for tooth identification but does not always yield fully consensus-based results. In this context, the use of additional quantitative methods becomes valuable. Morphometric techniques are widely applied to identify isolated theropod teeth and differentiate species (Alonso et al., 2018; Averianov et al., 2019; Buckley et al., 2010; Fanti & Therrien, 2007; Gates et al., 2013; Hendrickx et al., 2023; Larson & Currie, 2013; Torices et al., 2014; Williamson & Brusatte, 2014). 3D GMM, in particular, helps justify groupings and identify potential inaccuracies. However, comparative anatomy remains essential for post hoc verification. In our study, these methods can be applied to analyze isolated sauropod teeth and to assess heterodonty. Machine learning techniques are increasingly being proposed for the study of isolated teeth (Hendrickx et al., 2023; Wills et al., 2021, 2023). Among these, unsupervised clustering performs poorly, while semi-supervised and supervised clustering produce results comparable to those of comparative anatomy. The poor performance of unsupervised and semi-supervised classifications can be attributed to several biases. These include, in particular, the lack of data on certain fossils due to taphonomy, which requires data imputation, as well as the morphological continuity between the teeth in the jaw (Hendrickx et al., 2023; Wills et al., 2021, 2023). Nevertheless, these methods enable tooth reassessment and comparison, helping to resolve non-consensual determinations. Previous studies have demonstrated that combining different approaches with rigorous training in classification (Wills et al., 2023) is the most effective method for identifying isolated theropod teeth, achieving a taxonomic accuracy of 96% (Hendrickx et al., 2023). Additionally, Wills et al. (2023), as cited by Hendrickx et al. (2023), hypothesized that this multidisciplinary approach could reveal heterodonty. The strong performance of method combination in our study supports this hypothesis, further validating the findings of Wills et al. (2023) and Hendrickx et al. (2023). It is important to point out, however, that AI methods in paleontology remain challenging to implement, at least because they require training and learning data to be able to carry out the required analyses, and the number of usable fossil specimens is very limited, notably due to preservation biases and taphonomic effects (Yu et al., 2024). The large amount of data required to train AI is very complicated to collect in paleontology, and a great deal of supervisory work needs to be done by the operators (Yu et al., 2024). It is important to bear in mind that the use of multiple methods such as 3D GMM and clustering remains dependent on the comparative anatomy work carried out upstream.

In terms of time efficiency, comparative anatomy remains a relatively fast method. Each operator took approximately 7–8 h to classify all of the teeth. In contrast, quantitative methods require significantly more time, particularly in data preparation and acquisition. Fossil scanning and 3D file processing take approximately 10–15 min per specimen. Sometimes this step is not possible because not all researchers necessarily have the resources to obtain scanning equipment. Additionally, placing landmarks for geometric morphometrics requires careful attention, with around 5 min needed per fossil. Finally, the various analyses conducted in RStudio take between 1 and 1.5 days, including the time required to set up the corresponding scripts. For obtaining quick and reliable results, comparative anatomy is the most efficient approach; however, for more rigorous and comprehensive outcomes, combining qualitative and quantitative methods remains essential.

This study therefore allows for the reliable assignment of teeth to specific regions or jaw positions in turiasaur sauropods. Such assignment work is also necessary for many other non-mammalian

taxa, but studies dedicated to this topic are rare (Fruchard, 2012; Hendrickx et al., 2023; Wills et al., 2021, 2023). Given its highly satisfactory results, this method will therefore be useful for future research. Indeed, it is fully applicable to other sauropod taxa, such as Camarasauridae, or sauropods having large crown teeth (Le Gouellec et al., 2026). In theropods, the vast majority of geometric morphometric analyses have been conducted in 2D (Alonso et al., 2018; Averianov et al., 2019; Buckley et al., 2010; Fanti & Therrien, 2007; Gates et al., 2013; Hendrickx et al., 2023; Larson & Currie, 2013; Torices et al., 2014; Williamson & Brusatte, 2014). Incorporating a 3D method, as we have done here, should significantly improve the results of these analyses. Taxa other than dinosaurs, such as crocodilians, could also be analyzed using this methodology (Buffetaut, 1975; Carvalho, 1993, 1994; Prasad & Lapparent De Broin, 2002).

5 | CONCLUSION

In this study, we identified multiple dental morphotypes that justify heterodonty in the turiasaurian from Angeac-Charente (Charente, France) using various qualitative and quantitative methods. This sauropod exhibits dental morphological groups: premaxillary, anterior maxillary, posterior maxillary, anterior dentary, and posterior dentary teeth. The middle teeth are more suggestive and difficult to determine. To achieve this, we employed three methods and found them to be complementary in determining morphotypes and classifying teeth. Comparative anatomy proved to be the fastest method, yielding highly satisfactory results despite occasional operator-related discrepancies. In contrast, 3D geometric morphometrics demonstrated high efficiency but required significantly more labor-intensive data acquisition and processing. Thus, previously conflicting teeth are no longer ambiguous when analyzed by geometric morphometry and supervised classification. This highlights the usefulness of combining comparative anatomy, classifications, and geometric morphometrics to obtain more comprehensive and robust classification results. When combined with comparative anatomy and machine learning using supervised classification, this approach completely resolves conflicts in morphotype identification. Semi-supervised classification algorithms produced results similar to those obtained through comparative anatomy, whereas unsupervised classification algorithms failed to yield any conclusive results. Therefore, a multi-methodological approach is necessary for this study. Additionally, it is important to consider that other machine learning methods, such as Random Forest or C4.5 algorithms, should be tested, as they may provide different results. Finally, this multi-methodological approach is entirely applicable to other reptilian groups such as crocodilians or theropod dinosaurs.

AUTHOR CONTRIBUTIONS

Clémence Le Gouellec: Conceptualization, comparative anatomy and classification, formal analysis, investigation, writing original draft, writing—review and editing. **Ronan Allain:** Conceptualization, comparative anatomy and classification, resources, funding acquisition, writing—review and editing. **Jean Goedert:** Conceptualization, comparative anatomy and classification, funding acquisition, writing—review and editing. **Romain Pintore:** Comparative anatomy and classification, writing—review and editing. **Jackson Carter:** Writing—review and editing. **Rafael Royo-Torres:** Comparative anatomy and classification, writing—review and editing. **Dominique Augier:** Comparative anatomy and classification, writing—review and editing. **Raphaël Cornette:** Conceptualization, writing—review and editing.

ACKNOWLEDGMENTS

The authors thank F. Goussard (CR2P) and N. Poulet-Crovisier (CR2P) for all of the 3D surface scans of the teeth. The authors also thank L. Cazes (CR2P) for all of the photographs of teeth used to create the anatomical plates. The authors also thank the curator of the Angoulême Museum, L. Crépin, for welcoming them to study the sauropod dental material from Angeac-Charente and for the authorization to loan certain specimens. The authors also thank G. Bailly and P. Gruel, volunteers at the Angoulême Museum, for their participation and assistance in classifying the teeth. The authors would also like to thank V. Fernandez (ESRF) and N. Poulet-Crovisier (CR2P) for carrying out the scan and X-ray computed microtomography of the turiasaur left partial maxilla at the ESRF in Grenoble (proposal LS3173). The authors would like to thank Francette Rodet, the Audoin & Fils company, and the department of La Charente for donating all of the fossil material discovered at Angeac-Charente to the Angoulême museum. We thank the department of La Charente, the community of communes of the Châteauneuf region, and the community of agglomeration of Grand Cognac for their financial support. The authors thank Hélène Brisson and all of the inhabitants of Angeac-Charente for welcoming them every summer since 2011. Finally, The authors would like to thank all of the volunteers who have participated in Angeac-Charente dig campaigns, which have taking place every summer since August 2010. The authors also thank DIM MAP and ARS CUTTOLI, PAUL APPELL Foundation obtained by J Goedert this study, and the Fundación Conjunto Paleontológico de Teruel-Dinópolis and University of Zaragoza which funded Rafael Royo-Torres for the field campaigns from 2015 to 2019 and 2021–2025 at the Angeac-Charente site, respectively. Open access publication funding provided by COUPERIN CY26.

CONFLICTS OF INTEREST STATEMENT

The authors declare no conflicts of interest.

DATA AVAILABILITY STATEMENT

The original contributions presented in the study are included in the article/supporting information. Further inquiries can be directed to the corresponding author.

ORCID

Clémence L. E. Gouellec https://orcid.org/0009-0009-7765-4671
Ronan Allain https://orcid.org/0000-0002-6357-1586
Romain Pintore https://orcid.org/0000-0003-2438-614X

on heterodonty and rostrum shape. *The Anatomical Record*, 308, 1331–1348. Available from: https://doi.org/10.1002/ar.25563

De Brito, L. & Prestianni, C. (2021) *Pityostrobus andraei* (Pinaceae) from the Barremian (lower cretaceous) of Belgium: a morphometric revision. *International Journal of Plant Sciences*, 182(3), 174–184. Available from: https://doi.org/10.1086/712355

D'Emic, M.D., Whitlock, J.A., Smith, K.M., Fisher, D.C. & Wilson, J.A. (2013) Evolution of high tooth replacement rates in sauropod dinosaurs. *PLoS One*, 8(7), e69235. Available from: https://doi.org/10.1371/journal.pone.0069235

Deo, R.C. (2015) Machine learning in medicine. *Circulation*, 132(20), 1920–1930. Available from: https://doi.org/10.1161/circulationaha.115.001593

Ereshefsky, M. (1997) The evolution of the Linnaean hierarchy. *Biology & Philosophy*, 12(4), 493–519. Available from: https://doi.org/10.1023/A:1006556627052

Erickson, G.M., Gignac, P.M., Lappin, A.K., Vliet, K.A., Brueggen, J.D. & Webb, G.J.W. (2014) A comparative analysis of ontogenetic bite-force scaling among C rocodylia. *Journal of Zoology*, 292(1), 48–55. Available from: https://doi.org/10.1111/jzo.12081

Erickson, G.M., Gignac, P.M., Steppan, S.J., Lappin, A.K., Vliet, K.A. & Brueggen, J.D. (2012) Insights into the ecology and evolutionary success of crocodilians revealed through bite-force and tooth-pressure experimentation. *PLoS One*, 7(3), e31781. Available from: https://doi.org/10.1371/journal.pone.0031781

Fanti, F. & Therrien, F. (2007) Theropod tooth assemblages from the late cretaceous Maevarano formation and the possible presence of dromaeosaurids in Madagascar. *Acta Palaeontologica Polonica*, 52(1), 155–166.

Farber, P.L. (1975) Buffon and Daubenton: divergent traditions within the Histoire naturelle. *Isis*, 66(1), 63–74.

Farlow, J.O. & Brinkman, D.L. (1994) Wear surfaces on the teeth of tyrannosaurs. *The Paleontological Society Special Publications*, 7, 165–176. Available from: https://doi.org/10.1017/S2475262200009503

Farlow, J.O., Brinkman, D.L., Abler, W.L. & Currie, P.J. (1991) Size, shape, and serration density of theropod dinosaur lateral teeth. *Modern Geology*, 16(1–2), 161–198.

Feltes, B.C., Grisci, B.I., Poloni, J.D.F. & Dorn, M. (2018) Perspectives and applications of machine learning for evolutionary developmental biology. *Royal Society of Chemistry (RSC)*, 14(5), 289–306. Available from: https://doi.org/10.1039/c8mo00111a

Ferrón, H.G., Greenwood, J.M., Deline, B., Martínez-Pérez, C., Botella, H. & Sansom, R.S. (2020) Categorical versus geometric morphometric approaches to characterizing the evolution of morphological disparity in Osteostraci (vertebrata, stem Gnathostomata). *Palaeontology*, 63(5), 717–732. Available from: https://doi.org/10.1111/pala.12482

Foster, J.R., Woodruff, D.C. & Royo-Torres, R. (2026) The first evidence of Turiasauria (Sauropoda) in the upper Jurassic Morrison formation. *New Mexico Museum of Natural History & Science Bulletin*, 102, 267–282.

Frauenfelder, T.G., Birch, S.A., Bell, P.R. & Campione, N.E. (2024) Revealing the use of dental indices to infer taxonomic variation in sauropod dinosaurs. *Palaeontology*, 67(5), e12725. Available from: https://doi.org/10.1111/pala.12725

Fruchard, C. (2012) The Nile crocodile, a new model for investigating heterodonty and dental continuous renewal in vertebrates. *BioSciences Master Reviews*, 10, 1–10.

Gates, T.A., Zanno, L.E. & Makovicky, P.J. (2013) Theropod teeth from the upper Maastrichtian Hell Creek formation "sue" quarry: new morphotypes and faunal comparisons. *Acta Palaeontologica Polonica*, 60, 131–139. Available from: https://doi.org/10.4202/app.2012.0145

Gignac, P.M. & Erickson, G.M. (2014) Ontogenetic changes in dental form and tooth pressures facilitate developmental niche shifts in American alligators. *Journal of Zoology*, 295(2), 132–142. Available from: https://doi.org/10.1111/jzo.12187

Gomes Rodrigues, H., Cornette, R., Clavel, J., Cassini, G., Bhullar, B.-A.S., Fernández-Monescillo, M. et al. (2018) Differential influences of allometry, phylogeny and environment on the rostral shape diversity of extinct south American notoungulates. *Royal Society Open Science*, 5(1), 171816. Available from: https://doi.org/10.1098/rsos.171816

Goyal, S. (2022) Handling class-imbalance with KNN (Neighbourhood) under-sampling for software defect prediction. *Artificial Intelligence Review*, 55(3), 2023–2064. Available from: https://doi.org/10.1007/s10462-021-10044-w

Greener, J.G., Kandathil, S.M., Moffat, L. & Jones, D.T. (2022) A guide to machine learning for biologists. *Nature Reviews Molecular Cell Biology*, 23(1), 40–55. Available from: https://doi.org/10.1038/s41580-021-00407-0

Gunz, P. & Mitteroecker, P. (2013) Semilandmarks: a method for quantifying curves and surfaces. *Hystrix, the Italian Journal of Mammalogy*, 24(1), 103–109. Available from: https://doi.org/10.4404/hystrix-24.1-6292

Gunz, P., Mitteroecker, P. & Bookstein, F.L. (2005) Semilandmarks in three dimensions. In: Slice, D.E. (Ed.) *Modern morphometrics in physical anthropology, developments in primatology: Progress and prospects*. New York: Kluwer Academic Publishers-Plenum Publishers, pp. 73–98. Available from: https://doi.org/10.1007/0-387-27614-9_3

Gunz, P., Mitteroecker, P., Neubauer, S., Weber, G.W. & Bookstein, F.L. (2009) Principles for the virtual reconstruction of hominin crania. *Journal of Human Evolution*, 57(1), 48–62. Available from: https://doi.org/10.1016/j.jhevol.2009.04.004

Hendrickx, C. & Mateus, O. (2014) Abelisauridae (Dinosauria: Theropoda) from the late Jurassic of Portugal and dentition-based phylogeny as a contribution for the identification of isolated theropod teeth. *Zootaxa*, 3759(1), 1–74. Available from: https://doi.org/10.11646/zootaxa.3759.1.1

Hendrickx, C., Mateus, O. & Araújo, R. (2015a) The dentition of Megalosauridae (Theropoda: Dinosauria). *Acta Palaeontologica Polonica*, 60, 627. Available from: https://doi.org/10.4202/app.00056.2013

Hendrickx, C., Mateus, O. & Araújo, R. (2015b) A proposed terminology of theropod teeth (Dinosauria, Saurischia). *Journal of Vertebrate Paleontology*, 35(5), e982797. Available from: https://doi.org/10.1080/02724634.2015.982797

Hendrickx, C., Trapman, T.H., Wills, S., Holwerda, F.M., Stein, K.H.W. & Rauhut, O.W.M. (2023) A combined approach to identify isolated theropod teeth from the Cenomanian Kem Group of Morocco: cladistic, discriminant, and machine learning analyses. *Journal of Vertebrate Paleontology*, 43(4), e2311791. Available from: https://doi.org/10.1080/02724634.2024.2311791

Hendrickx, C., Tschopp, E. & Ezcurra, M.D. (2020) Taxonomic identification of isolated theropod teeth: the case of the shed tooth crown associated with Aerosteon (Theropoda: Megaraptora) and the dentition of Abelisauridae. *Cretaceous Research*, 108, 104312. Available from: https://doi.org/10.1016/j.cretres.2019.104312

Holwerda, F.M., Pol, D. & Rauhut, O.W.M. (2015) Using dental enamel wrinkling to define sauropod tooth morphotypes from the Cañadón Asfalto formation, Patagonia, Argentina. *PLoS One*, 10(2), e0118100. Available from: https://doi.org/10.1371/journal.pone.0118100

Hou, C., Lin, X., Huang, H., Xu, S., Fan, J., Shi, Y., et al. (2023) Fossil image identification using deep learning ensembles of data augmented multiviews. *Methods inEcology and Evolution*, 14, 3020–3034. Available from: https://doi.org/10.1111/2041-210X.14229

Kardong, K.V. (2006) *Vertebrates: comparative anatomy, function, evolution*. New York: McGraw-Hill.

Kaya, Y., Pınar, S.M., Erez, M.E. & Fidan, M. (2013) An expert classification system of pollen of Onopordum using a rough set approach. *Review of Palaeobotany and Palynology*, 189, 50–56. Available from: https://doi.org/10.1016/j.revpalbo.2012.11.004

Kieser, J.A., Klapsidis, C., Law, L. & Marion, M. (1993) Heterodonty and patterns of tooth replacement in *Crocodylus niloticus*. *Journal of Morphology*, 218(2), 195–201. Available from: https://doi.org/10.1002/jmor.1052180208

Klingenberg, C.P. (2010) Evolution and development of shape: integrating quantitative approaches. *Nature Reviews Genetics*, 11(9), 623–635. Available from: https://doi.org/10.1038/nrg2829

Klingenberg, C.P. (2013) Visualizations in geometric morphometrics: how to read and how to make graphs showing shape changes. *Hystrix, the Italian Journal of Mammalogy*, 24(1), 15. Available from: https://doi.org/10.4404/hystrix-24.1-7691

Klingenberg, C.P. & Monteiro, L.R. (2005) Distances and directions in multidimensional shape spaces: implications for morphometric applications. *Systematic Biology*, 54(4), 678–688. Available from: https://doi.org/10.1080/10635150590947258

Kobayashi, Y. & Azuma, Y. (2003) A new iguanodontian (Dinosauria: Ornithopoda) from the lower cretaceous Kitadani formation of Fukui prefecture, Japan. *Journal of Vertebrate Paleontology*, 23(1), 166–175.

Korteling, J.E.(H.), Van De Boer-Visschedijk, G.C., Blankendaal, R.A.M., Boonekamp, R.C. & Eikelboom, A.R. (2021) Human- versus Artificial Intelligence. *Frontiers in Artificial Intelligence*, 4, 622364. Available from: https://doi.org/10.3389/frai.2021.622364

Kuzenkov, O., Morozov, A. & Kuzenkova, G. (2020) Exploring evolutionary fitness in biological systems using machine learning methods. *Entropy*, 23(1), 35. Available from: https://doi.org/10.3390/e23010035

Lafuma, F., Corfe, I.J., Clavel, J. & Di-Poï, N. (2021) Multiple evolutionary origins and losses of tooth complexity in squamates. *Nature Communications*, 12(1), 6001. Available from: https://doi.org/10.1038/s41467-021-26285-w

Lallensack, J.N., Romilio, A. & Falkingham, P.L. (2022) A machine learning approach for the discrimination of theropod and ornithischian dinosaur tracks. *Journal of the Royal Society Interface*, 19(196), 20220588. Available from: https://doi.org/10.1098/rsif.2022.0588

Langston, W. (1973) The Crocodilian skull in Historical Perspective. *Biology of the Reptilia*, 4, 263.

Larson, D.W. & Currie, P.J. (2013) Multivariate analyses of small theropod dinosaur teeth and implications for Paleoecological turnover through time. *PLoS One*, 8(1), e54329. Available from: https://doi.org/10.1371/journal.pone.0054329

Larsson, H.C.E. & Sidor, C.A. (1999) Unusual crocodyliform teeth from the late cretaceous (Cenomanian) of southeastern Morocco. *Journal of Vertebrate Paleontology*, 19(2), 398–401. Available from: https://doi.org/10.1080/02724634.1999.10011152

Lawing, A.M. & Polly, P.D. (2010) Geometric morphometrics: recent applications to the study of evolution and development. *Journal of Zoology*, 280(1), 1–7. Available from: https://doi.org/10.1111/j.1469-7998.2009.00620.x

Le Gouellec, C., Goedert, J., Cobos, A., Royo-Torres, R. & Allain, R. (2026) Variation intra et interspécifique des dents de sauropodes d'Angeac-Charente. https://doi.org/10.13140/RG.2.2.10008.76806/1

Lê, S., Josse, J. & Husson, F. (2008) FactoMineR: an *R* package for multivariate analysis. *Journal of Statistical Software*, 25(1), 1–18. Available from: https://doi.org/10.18637/jss.v025.i01

Liao, C.-C., Moore, A., Jin, C., Yang, T.-R., Shibata, M. & Jin, F. (2021) A possible brachiosaurid (Dinosauria, Sauropoda) from the mid-cretaceous of northeastern China. *PeerJ*, 9, e11957. Available from: https://doi.org/10.7717/peerj.11957

Linnaei, C. (1735) *Systema naturae, sive regna tria naturae systematice proposita per classes, ordines, genera, & species*. Lugduni Batavorum: Apud Theodore Haak: Ex Typographia Joannis Wilhelmi de Groot. usdanationalagriculturallibrary; fedlink.

Liu, S., Thonnat, M. & Berthod, M. (1994) Automatic classification of planktonic foraminifera by a knowledge-based system. In: *Proceedings of the tenth conference on artificial intelligence for applications. Presented at the tenth conference on artificial intelligence for applications*. San Antonia, TX, USA: IEEE, pp. 358–364. Available from: https://doi.org/10.1109/CAIA.1994.323653

Liu, X., Jiang, S., Wu, R., Shu, W., Hou, J., Sun, Y. (2023) Automatic taxonomic identification based on the Fossil Image Dataset (>415,000 images) and deep convolutional neural networks. *Paleobiology*, 49(1), 1–22. Available from: https://doi.org/10.1017/pab.2022.14

Livezey, B.C. & Zusi, R.L. (2001) Higher-order phylogenetics of modern aves based on comparative anatomy. *Netherlands Journal of Zoology*, 51(2), 179–205. Available from: https://doi.org/10.1163/156854201750385145

Lürig, M.D., Donoughe, S., Svensson, E.I., Porto, A. & Tsuboi, M. (2021) Computer vision, machine learning, and the promise of phenomics in ecology and evolutionary biology. *Frontiers in Ecology and Evolution*, 9, 1–19. Available from: https://doi.org/10.3389/fevo.2021.642774

Maier, W. (1984) Tooth morphology and dietary specialization. In: *Food acquisition and processing in primates*. Boston, MA: Springer US, pp. 303–330. Available from: https://doi.org/10.1007/978-1-4757-5244-1_13

Maiorino, L., Farke, A.A., Kotsakis, T., Teresi, L. & Piras, P. (2015) Variation in the shape and mechanical performance of the lower jaws in ceratopsid dinosaurs (Ornithischia, Ceratopsia). *Journal of Anatomy*, 227(5), 631–646. Available from: https://doi.org/10.1111/joa.12374

Mallon, J.C. & Anderson, J.S. (2014) The functional and palaeoecological implications of tooth morphology and Wear for the Megaherbivorous dinosaurs from the Dinosaur Park formation (upper Campanian) of Alberta, Canada. *PLoS One*, 9(6), e98605. Available from: https://doi.org/10.1371/journal.pone.0098605

Mannion, P.D., Allain, R. & Moine, O. (2017) The earliest known titanosauriform sauropod dinosaur and the evolution of Brachiosauridae. *PeerJ*, 5, e3217.

Mateus, O., Mannion, P.D. & Upchurch, P. (2014) *Zby atlanticus*, a new turiasaurian sauropod (Dinosauria, Eusauropoda) from the late Jurassic of Portugal. *Journal of Vertebrate Paleontology*, 34(3), 618–634. Available from: https://doi.org/10.1080/02724634.2013.822875

Melstrom, K.M. (2017) The relationship between diet and tooth complexity in living dentigerous saurians: MELSTROM-SAURIAN DENTAL COMPLEXITY AND DIET. *Journal of Morphology*, 278(4), 500–522. Available from: https://doi.org/10.1002/jmor.20645

Milàn, J. & Mateus, O. (2023) A turiasaurian (Dinosauria, Sauropoda) tooth from the Pliensbachian Hasle formation of Bornholm, Denmark, shows an early Jurassic origin of the Turiasauria. *Diversity*, 16(1), 12. Available from: https://doi.org/10.3390/d16010012

Mocho, P., Royo-Torres, R., Malafaia, E., Escaso, F. & Ortega, F. (2017) Sauropod tooth morphotypes from the upper Jurassic of the Lusitanian Basin (Portugal). *Papers in Palaeontology*, 3(2), 259–295. Available from: https://doi.org/10.1002/spp2.1075

Mocho, P., Royo-Torres, R., Malafaia, E., Escaso, F., Silva, B. & Ortega, F. (2016) Turiasauria-like teeth from the upper Jurassic of the Lusitanian Basin, Portugal. *Historical Biology*, 28(7), 861–880. Available from: https://doi.org/10.1080/08912963.2015.1049948

Moore, A.J., Mo, J., Clark, J.M. & Xu, X. (2018) Cranial anatomy of *Bellusaurus sui* (Dinosauria: Eusauropoda) from the middle-late Jurassic Shishugou formation of northwest China and a review of sauropod cranial ontogeny. *PeerJ*, 6, e4881. Available from: https://doi.org/10.7717/peerj.4881

Nabavizadeh, A. (2023) How *Triceratops* got its face: an update on the functional evolution of the ceratopsian head. *The Anatomical*

Record, 306(7), 1951–1968. Available from: https://doi.org/10.1002/ar.25196

Néraudeau, D., Allain, R., Ballèvre, M., Batten, D.J., Buffetaut, E. & Colin, J.P. (2012) The Hauterivian–Barremian lignitic bone bed of Angeac (Charente, south-west France): stratigraphical, palaeobiological and palaeogeographical implications. *Cretaceous Research*, 37, 1–14. Available from: https://doi.org/10.1016/j.cretres.2012.01.006

Nieuwland, I. (2024) The first fossil collectors dinosaurs at the dinner party Edward Dolnick Scribner. *Science*, 385(6707), 375. Available from: https://doi.org/10.1126/science.adq5704

Norman, D.B., Crompton, A.W., Butler, R.J., Porro, L.B. & Charig, A.J. (2011) The lower Jurassic ornithischian dinosaur Heterodontosaurus tucki Crompton & Charig, 1962: cranial anatomy, functional morphology, taxonomy, and relationships. *Zoological Journal of the Linnean Society*, 163, 182–276. Available from: https://doi.org/10.1111/j.1096-3642.2011.00697.x

Osborn, H.F. (1905) Tyrannosaurus and other cretaceous carnivorous dinosaurs. *Proceedings of the Academy of Natural Sciences of Philadelphia*, 8, 72.

Osborn, J.W. (1998) Relationship between growth and the pattern of tooth initiation in alligator embryos. *Journal of Dental Research*, 77(9), 1730–1738. Available from: https://doi.org/10.1177/00220345980770090901

Ostrom, J.H. (1966) Functional morphology and evolution of the ceratopsian dinosaurs. *Evolution*, 20(3), 290. Available from: https://doi.org/10.2307/2406631

Owen, R. (1846) *A history of British fossil mammals, and birds*. Cambridge: Cambridge University Press.

Pintore, R., Cornette, R., Houssaye, A. & Allain, R. (2023) Femora from an exceptionally large population of coeval ornithomimosaurs yield evidence of sexual dimorphism in extinct theropod dinosaurs. *eLife*, 12, e83413. Available from: https://doi.org/10.7554/eLife.83413

Porz, N., Habegger, S., Meier, R., Verma, R., Jilch, A. & Fichtner, J. (2016) Fully automated enhanced tumor compartmentalization: man vs. machine reloaded. *PLoS One*, 11(11), e0165302. Available from: https://doi.org/10.1371/journal.pone.0165302

Prasad, G.V.R. & Lapparent De Broin, F. (2002) Late cretaceous crocodile remains from Naskal (India): comparisons and biogeographic affinities. *Annales de Paleontologie*, 88(1), 19–71. Available from: https://doi.org/10.1016/S0753-3969(02)01036-4

Quinlan, J.R. (2014) *C4. 5: programs for machine learning*. Amsterdam: Elsevier.

R Core Team. (2022) R: A language and environment for statistical computing.

Rajathi, S. & Radhamani, G. (2016) Prediction and analysis of rheumatic heart disease using kNN classification with ACO. In: *2016 international conference on data mining and advanced computing (SAPIENCE). Presented at the 2016 international conference on data mining and advanced computing (SAPIENCE)*. Ernakulam, India: IEEE, pp. 68–73. Available from: https://doi.org/10.1109/SAPIENCE.2016.7684132

Rajkomar, A., Dean, J. & Kohane, I. (2019) Machine learning in medicine. *New England Journal of Medicine*, 380(14), 1347–1358. Available from: https://doi.org/10.1056/NEJMra1814259

Régent, V., Wiersma-Weyand, K., Wings, O., Knötschke, N. & Sander, P.M. (2024) The dentition of the late Jurassic dwarf sauropod *Europasaurus holgeri* from northern Germany: ontogeny, function, and implications for a rhamphotheca-like structure in Sauropoda. *PeerJ*, 12, e17764. Available from: https://doi.org/10.7717/peerj.17764

Reichel, M. (2010a) A model for the bite mechanics in the herbivorous dinosaur stegosaurus (Ornithischia, Stegosauridae). *Swiss Journal of Geosciences*, 103(2), 235–240. Available from: https://doi.org/10.1007/s00015-010-0025-1

Reichel, M. (2010b) The heterodonty of *Albertosaurus sarcophagus* and *tyrannosaurus rex*: biomechanical implications inferred through 3-D modelsThis article is one of a series of papers published in this special issue on the theme *Albertosaurus*. *Canadian Journal of Earth Sciences*, 47(9), 1253–1261. Available from: https://doi.org/10.1139/E10-063

Ribeiro, M., Mocho, P. & Pereira, S. (2024) Application of multivariate morphometry to access the morphological variability in sauropod teeth. *Zubía*, 42, 209–214.

Ribeiro Relvas, M.E. (2023) *Testing the application of multivariate morphometrics to quantify and classify morphological variability in sauropod dinosaur teeth*. Portugal: University of Coimbra.

Robin, O., Cornette, R. & Clavel, B. (2023) Distinguishing female, male and castrated sheep using linear metrics and geometric morphometrics: application on an archaeological assemblage. *Journal of Archaeological Science: Reports*, 51, 104225. Available from: https://doi.org/10.1016/j.jasrep.2023.104225

Rogers, K.C. & Wilson, J. (2005) *The sauropods: evolution and paleobiology*. California: University of California Press.

Rohlf, F.J. & Slice, D. (1990) Extensions of the Procrustes method for the optimal superimposition of landmarks. *Systematic Biology*, 39(1), 40–59. Available from: https://doi.org/10.2307/2992207

Royo-Torres, R., Cobos, A. & Alcalá, L. (2006) A Giant European dinosaur and a new sauropod clade. *Science*, 314(5807), 1925–1927. Available from: https://doi.org/10.1126/science.1132885

Royo-Torres, R., Cobos, A., Mocho, P. & Alcalá, L. (2021) Origin and evolution of turiasaur dinosaurs set by means of a new rosetta specimen from Spain. *Zoological Journal of the Linnean Society*, 191(1), 201–227. Available from: https://doi.org/10.1093/zoolinnean/zlaa091

Royo-Torres, R. & Upchurch, P. (2012) The cranial anatomy of the sauropod *Turiasaurus riodevensis* and implications for its phylogenetic relationships. *Journal of Systematic Palaeontology*, 10(3), 553–583. Available from: https://doi.org/10.1080/14772019.2011.598577

Royo-Torres, R., Upchurch, P., Kirkland, J.I., DeBlieux, D.D., Foster, J.R., Cobos, A. et al. (2017) Descendants of the Jurassic turiasaurs from Iberia found refuge in the early cretaceous of western USA. *Scientific Reports*, 7(1), 14311. Available from: https://doi.org/10.1038/s41598-017-14677-2

Rozada, L., Allain, R., Vullo, R., Goedert, J., Augier, D. & Jean, A. (2021) A lower cretaceous *Lagerstätte* from France: a taphonomic overview of the Angeac-Charente vertebrate assemblage. *Lethaia*, 54(2), 141–165. Available from: https://doi.org/10.1111/let.12394

Saleiro, A. & Tschopp, E. (2025) New sauropod teeth from the upper Jurassic of Portugal and their implications for sauropod dental evolution. *Papers in Palaeontology*, 11(1), e70001. Available from: https://doi.org/10.1002/spp2.70001

Schlager, S. (2017) Morpho and Rvcg – shape analysis in R. In: *Statistical shape and deformation analysis*. Amsterdam: Elsevier, pp. 217–256. Available from: https://doi.org/10.1016/B978-0-12-810493-4.00011-0

Schmieder, D.A., Benítez, H.A., Borissov, I.M. & Fruciano, C. (2015) Bat species comparisons based on external morphology: a test of traditional versus geometric morphometric approaches. *PLoS One*, 10(5), e0127043. Available from: https://doi.org/10.1371/journal.pone.0127043

Scrucca, L., Fraley, C., Murphy, T.B. & Adrian E, R. (2023) *Model-based clustering, classification, and density estimation using mclust in R*, 1st edition. Boca Raton: Chapman and Hall/CRC. Available from: https://doi.org/10.1201/9781003277965

Segall, M., Houssin, C., Delapré, A., Cornette, R., Herrel, A. & Milgram, J. (2023) Armed to the teeth: the underestimated diversity in tooth shape in snakes and its relation to feeding behavior and diet. *Ecology and Evolution*, 13(4), e10011. Available from: https://doi.org/10.1002/ece3.10011

Sereno, P. (2012) Taxonomy, morphology, masticatory function and phylogeny of heterodontosaurid dinosaurs. *ZooKeys*, 226, 1–225. Available from: https://doi.org/10.3897/zookeys.226.2840

Sereno, P.C., Wilson, J.A., Witmer, L.M., Whitlock, J.A., Maga, A., Ide, O. et al. (2007) Structural Extremes in a Cretaceous Dinosaur. *PLoS One*, 2(11), e1230. Available from: https://doi.org/10.1371/journal.pone.0001230

Sereno, P.C. & Zhimin, D. (1992) The skull of the basal stegosaur *Huayangosaurus taibaii* and a cladistic diagnosis of stegosauria. *Journal of Vertebrate Paleontology*, 12(3), 318–343. Available from: https://doi.org/10.1080/02724634.1992.10011463

Sharma, A., Singh, S. & Satheesh, S.R. (2022) The first turiasaurian sauropod of India reported from the middle Jurassic (Bathonian) sediments of Jaisalmer Basin, Rajasthan, India. *NJGPA*, 304(2), 187–203. Available from: https://doi.org/10.1127/njgpa/2022/1064

Sidey-Gibbons, J.A.M. & Sidey-Gibbons, C.J. (2019) Machine learning in medicine: a practical introduction. *BMC Medical Research Methodology*, 19(1), 64. Available from: https://doi.org/10.1186/s12874-019-0681-4

Silverman, B.W. & Jones, M.C. (1989) E. Fix and J.L. Hodges (1951): an important contribution to nonparametric discriminant analysis and density estimation: commentary on fix and Hodges (1951). *International Statistical Review / Revue Internationale de Statistique*, 57(3), 233. Available from: https://doi.org/10.2307/1403796

Slice, D.E. (2007) Geometric morphometrics. *Annual Review of Anthropology*, 36(1), 261–281. Available from: https://doi.org/10.1146/annurev.anthro.34.081804.120613

Smith, J.B. (2005) Heterodonty in *tyrannosaurus rex*: implications for the taxonomic and systematic utility of theropod dentitions. *Journal of Vertebrate Paleontology*, 25(4), 865–887.

Smith, J.B. (2007) Dental morphology and variation in *Majungasaurus crenatissimus* (Theropoda: Abelisauridae) from the late createous of Madagascar. *Journal of Vertebrate Paleontology*, 27(2), 103–126.

Smith, J.B., Vann, D.R. & Dodson, P. (2005) Dental morphology and variation in theropod dinosaurs: implications for the taxonomic identification of isolated teeth. *The Anatomical Record Part A: Discoveries in Molecular, Cellular, and Evolutionary Biology*, 285(2), 699–736. Available from: https://doi.org/10.1002/ar.a.20206

Thalamuthu, A., Mukhopadhyay, I., Zheng, X. & Tseng, G.C. (2006) Evaluation and comparison of gene clustering methods in microarray analysis. *Bioinformatics*, 22(19), 2405–2412. Available from: https://doi.org/10.1093/bioinformatics/btl406

Torcida Fernández-Baldor, F., Huerta, P., Puértolas-Pascual, E. & Canudo, J.I. (2024) New teeth of a basal macronarian (Sauropoda) from the Jurassic–cretaceous transition of Spain. *Journal of Iberian Geology*, 50(1), 27–39. Available from: https://doi.org/10.1007/s41513-023-00217-7

Torices, A., Reichel, M. & Currie, P.J. (2014) Multivariate analysis of isolated tyrannosaurid teeth from the Danek bonebed, horseshoe canyon formation, Alberta, Canada. *Canadian Journal of Earth Sciences*, 51(11), 1045–1051. Available from: https://doi.org/10.1139/cjes-2014-0072

Venables, W.N. & Ripley, B.D. (2002) Statistics complements to modern applied statistics with S Fourth edition.

Vullo, R., Allain, R. & Cavin, L. (2016) Convergent evolution of jaws between spinosaurid dinosaurs and pike conger eels. *Acta Palaeontologica Polonica*, 61, 825. Available from: https://doi.org/10.4202/app.00284.2016

White, T.E. (1958) The braincase of camarasaurus lentus (marsh). *Journal of Paleontology*, 32, 477–494.

Whitlock, J.A., Wilson, J.A. & Lamanna, M.C. (2010) Description of a nearly complete juvenile skull of *diplodocus* (Sauropoda: Diplodocoidea) from the late Jurassic of North America. *Journal of Vertebrate Paleontology*, 30(2), 442–457. Available from: https://doi.org/10.1080/02724631003617647

Wiersma, K. & Sander, P.M. (2016) The dentition of a well-preserved specimen of camarasaurus sp.: implications for function, tooth replacement, soft part reconstruction, and food intake. *Paläontologische Zeitschrift*, 91(1), 145–161. Available from: https://doi.org/10.1007/s12542-016-0332-6

Williamson, T.E. & Brusatte, S.L. (2014) Small theropod teeth from the late cretaceous of the San Juan Basin, northwestern New Mexico and their implications for understanding latest cretaceous dinosaur evolution. *PLoS One*, 9(4), e93190. Available from: https://doi.org/10.1371/journal.pone.0093190

Wills, S., Underwood, C.J. & Barrett, P.M. (2021) Learning to see the wood for the trees: machine learning, decision trees, and the classification of isolated theropod teeth. *Palaeontology*, 64(1), 75–99. Available from: https://doi.org/10.1111/pala.12512

Wills, S., Underwood, C.J. & Barrett, P.M. (2023) Machine learning confirms new records of maniraptoran theropods in middle Jurassic UK microvertebrate faunas. *Papers in Palaeontology*, 9(2), e1487. Available from: https://doi.org/10.1002/spp2.1487

Wilson, J.A. (2005) Redescription of the mongolian sauropod *nemegtosaurus mongoliensis* nowinski (dinosauria: Saurischia) and comments on late cretaceous sauropod diversity. *Journal of Systematic Palaeontology*, 3(3), 283–318. Available from: https://doi.org/10.1017/S1477201905001628

Woodruff, D.C., Barrett, P.M., Ouarhache, D., El Khanchoufi, A., Boumir, K. & Ech-Charay, K. (2025) Teeth from the middle Jurassic of Morocco reveal the oldest turiasaurian sauropods from Africa. *Acta Palaeontologica Polonica*, 70(3), 411–420. Available from: https://doi.org/10.4202/app.01214.2024

Yamanaka, A., Iwai, H., Uemura, M. & Goto, T. (2015) Patterning of mammalian heterodont dentition within the upper and lower jaws. *Evolution and Development*, 17(2), 127–138. Available from: https://doi.org/10.1111/ede.12116

Yang, K., Wu, J., Li, X., Pang, X., Yuan, Y., Qi, G. et al. (2022) Intraspecific leaf morphological variation in Quercus dentata Thunb: a comparison of traditional and geometric morphometric methods, a pilot study. *Journal of Forestry Research*, 33(6), 1751–1764. Available from: https://doi.org/10.1007/s11676-022-01452-x

Yu, C., Qin, F., Watanabe, A., Yao, W., Li, Y., Qin, Z. et al. (2024) Artificial intelligence in paleontology. *Earth-Science Reviews*, 252, 104765. Available from: https://doi.org/10.1016/j.earscirev.2024.104765

Zahradnicek, O., Buchtova, M., Dosedelova, H. & Tucker, A.S. (2014) The development of complex tooth shape in reptiles. *Frontiers in Physiology*, 5, 74. Available from: https://doi.org/10.3389/fphys.2014.00074

Zangerl, R. (1948) The methods of comparative anatomy and its contribution to the study of evolution. *Evolution*, 2(4), 351. Available from: https://doi.org/10.2307/2405524

Zelditch, M., Swiderski, D. & Sheets, H.D. (2012) *Geometric morphometrics for biologists: a primer*. Cambridge: Academic press.

SUPPORTING INFORMATION

Additional supporting information can be found online in the Supporting Information section at the end of this article.

How to cite this article: Gouellec, C.L.E., Allain, R., Goedert, J., Pintore, R., Carter, J., Royo-Torres, R. et al. (2026) Heterodonty in the teeth of the turiasaurian sauropod from Angeac-Charente (Early Cretaceous, southwestern France): Comparison of anatomical and geometric morphometric approaches. *Journal of Anatomy*, 00, 1–26. Available from: https://doi.org/10.1111/joa.70230